

General Disclaimer

One or more of the Following Statements may affect this Document

- This document has been reproduced from the best copy furnished by the organizational source. It is being released in the interest of making available as much information as possible.
- This document may contain data, which exceeds the sheet parameters. It was furnished in this condition by the organizational source and is the best copy available.
- This document may contain tone-on-tone or color graphs, charts and/or pictures, which have been reproduced in black and white.
- This document is paginated as submitted by the original source.
- Portions of this document are not fully legible due to the historical nature of some of the material. However, it is the best reproduction available from the original submission.

Report No. R-75-022
July 1975

FINAL REPORT
HIGH RELIABILITY BOND PROGRAM USING
SMALL DIAMETER ALUMINUM WIRE

by

Milo Macha
R. A. Thiel

Contract: **NAS8-30877**

Prepared by

General Dynamics Electronics Division
Microelectronics Center
Mail Zone 7-08

Prepared for

George C. Marshall Space Flight Center
Marshall Space Flight Center
Alabama 35312

GENERAL DYNAMICS
Electronics Division



(NASA-CR-143946) HIGH RELIABILITY BOND
PROGRAM USING SMALL DIAMETER ALUMINUM WIRE
Final Report (General Dynamics/Electronics)
CSC 13H
55 p HC \$4.25
G3/37 40323
Unclas
N75-32462

Report No. R-75-022
July 1975

FINAL REPORT
HIGH RELIABILITY BOND PROGRAM USING
SMALL DIAMETER ALUMINUM WIRE

by
Milo Macha
R. A. Thiel

Contract: ~~NAS8-30877~~
NAS8-30877

Prepared by
General Dynamics Electronics Division
Microelectronics Center
Mail Zone 7-08

Prepared for
George C. Marshall Space Flight Center
Marshall Space Flight Center
Alabama 35312

GENERAL DYNAMICS
Electronics Division

P.O. Box 81127, San Diego, California 92138 - 714-279-7301

CONTENTS

<u>Section</u>	<u>Page</u>
OVERVIEW	vi
ACKNOWLEDGEMENTS	vii
1 INTRODUCTION	1-1
2 APPROACH	2-1
2.1 Substrate and Wiring Pattern	2-1
2.2 Materials	2-3
2.2.1 Thick Film Gold	2-3
2.2.2 Thin Film Gold	2-4
2.2.3 Thin Film Aluminum	2-4
2.2.4 Bonding Wire	2-4
2.2.5 Semiconductor Components	2-4
2.3 Equipment	2-4
2.3.1 Vacuum Evaporator	2-5
2.3.2 Bonder and Ultrasonic Power Supply	2-7
2.3.3 Bonding Tools	2-12
2.3.4 Bonding Tool Inspection Fixture	2-13
2.3.5 Thermal Cycling Chamber	2-13
2.3.6 Other Equipment	2-15
2.4 Processes	2-17
2.4.1 Thick Film Gold Substrates	2-17
2.4.2 Thin Film Gold Substrates	2-17
2.4.3 Thin Film Aluminum Substrates	2-19
2.5 Data Analysis	2-19
3 DATA	3-1
3.1 Thick Film Only	3-1
3.2 Thick Film With Chips	3-1
3.3 Thin Film Only	3-2
3.4 Thin Film With Chips	3-2
3.5 Thin Film Aluminum	3-3
3.6 Bond Resistance	3-4

CONTENTS (Continued)

<u>Section</u>		<u>Page</u>
4	CONCLUSIONS	4-1
4.1	Thick Film Gold	4-2
4.2	Thin Film Gold	4-2
4.3	Chips	4-4
4.4	Thin Film Aluminum	4-5
5	RECOMMENDATIONS	5-1
6	REFERENCES	6-1

ILLUSTRATIONS

<u>Figure</u>	<u>Title</u>	<u>Page</u>
2-1	Substrate Pad Pattern	2-2
2-2	Wire Bond Test Pattern, Thick and Thin Film Gold	2-2
2-3	Wire Bond Test Pattern, Thin Film Aluminum	2-3
2-4	Vacuum Evaporator	2-6
2-5	Loading Vacuum Evaporator	2-6
2-6	Ultrasonic Bonder	2-7
2-7	First Bond Problem	2-9
2-8	Reset Problem	2-11
2-9	Bonder Timing	2-12
2-10	Tool Inspection Fixture	2-14
2-11	Thermal Shock Chamber	2-14
2-12	Wire Bond Pull Tester	2-16
2-13	Bonding Force Gage and Torque Wrench	2-16
2-14	Ultrasonic Bond Study, Thick Film Flow Chart	2-18
2-15	Ultrasonic Bonding Study, Thin Film Flow Chart	2-20
2-16	Ultrasonic Bonding Study, Al Thin Film Flow Chart	2-21
2-17	Calculator Printout	2-22
3-1	Wire Geometry	3-4
4-1	Wire Bonds (25.4 μ m)	4-3

TABLES

<u>Number</u>	<u>Title</u>	<u>Page</u>
2-1	1% Si-Al Wire	2-4
2-2	Ultrasonic Bonding Tools	2-13
3-1	Bond Strength Distribution, Thick Film Pattern, 25.4 μm (1 mil) Wire . . .	3-6
3-2	Bond Strength Distribution, Thick Film Pattern, 38.1 μm (1.5 mil) Wire .	3-7
3-3	Bond Strength Distribution, Thick Film Pattern, 50.8 μm (2 mil) Wire . . .	3-8
3-4	Bond Strength Distribution, Al Wire Bonded to Thick Film and Chips . . .	3-9
3-5	Bond Strength Distribution, Thin Film Pattern, 25.4 μm (1 mil) Wire . . .	3-10
3-6	Bond Strength Distribution, Thin Film Pattern, 38.1 μm (1.5 mil) Wire . .	3-11
3-7	Bond Strength Distribution, Thin Film Pattern, 50.8 μm (2 mil) Wire . . .	3-12
3-8	Bond Strength Distribution, Al Wire Bonded to Thin Film and Chips	3-13
3-9	Bond Strength Distribution, Al Wire Bonded to 1.6 μm Al Film	3-14
3-10	Electrical Resistance Data	3-15

OVERVIEW

The program was undertaken to characterize the performance of small diameter aluminum wire ultrasonically bonded to conductors commonly encountered in hybrid assemblies, and to recommend guidelines for improving this performance. 25.4, 38.1 and 50.8 μm (1, 1.5 and 2 mil) wire was used with bonding metallization consisting of thick film gold, thin film gold and aluminum as well as conventional aluminum pads on semiconductor chips. The chief tool for evaluating the performance was the double bond pull test in conjunction with a 72 hour - 150°C heat soak and -65°C to +150°C thermal cycling. In practice the thermal cycling was found to have relatively little effect compared to the heat soak.

In general, pull strength will decrease after heat soak as a result of annealing of the aluminum wire. When bonded to thick film gold, the pull strength decreased by about 50%. Even more important, weakening of the bond interface was the major cause of the reduction. Bonds to thin film gold lost about 30 - 40% of their initial pull strength but in this case, weakening of the wire itself at the bond heel was the predominant cause. Bonds to aluminum substrate metallization lost only about 22%. Bonds between thick and thin film gold substrate metallization and semiconductor chips substantiated the previous conclusions but also showed that in about 20 to 25% of the cases, bond interface failures occurred at the semiconductor chip.

Implementation of the NBS bonder calibration procedure is recommended as well as establishing a maximum 15% standard deviation and a minimum 5 gmf pull strength for 25.4 μm wire in hybrid geometries. Depending on requirements, evaluations should include the effect of wire hardness, substrate smoothness, metal thickness and impurities. A development program for a Ni/Cr aluminum hybrid process should be implemented. The most important recommendation is that a comparative study be made of the bondability of vendor supplied chips to provide guidelines for hybrid users.

ACKNOWLEDGEMENTS

The help of Joyce Gilliam in providing practical insights on the bonding process and her assistance with the establishment of bonding schedules is gratefully acknowledged. We also wish to thank Gerry Schmidt for his assistance in the business management of the program.

1. INTRODUCTION

The mechanism of ultrasonic bonding involves principles of metallurgical welding, surface physics, and solid state chemistry. Ultrasonic bonding like any other welding process is based upon the fact that metal atoms with unsatisfied bonds are capable of bonding to other atoms if they are brought into intimate contact. Atoms such as those adjacent to grain boundaries or at the surface have unsatisfied bonds and these bonds are responsible for adhesion of metal grains. If two pieces of metal with absolutely smooth, clean surfaces are brought together in intimate contact, the unsatisfied bonds of atoms on the surfaces of both pieces create a true metallurgical bond. However, if we consider the true nature of a clean, smooth metallic surface, it is evident that this kind of metallurgical bonding cannot normally occur. First, no matter how carefully a metal surface may be prepared, it is far from smooth on an atomic scale. A most carefully polished surface still has irregularities with peak-to-valley vertical distances that average about 5×10^{-6} cm, which corresponds to a distance of approximately 200 atomic layers. As the attractive forces between atoms with unsatisfied bonds decrease rapidly as the distance from the atom increases, only peaks can satisfy their bonds.

Real surfaces are not clean either. Oxygen molecules from air convert the surface atoms of the metal into oxide, which is approximately 200 molecules thick. At such thickness, the oxide has properties similar to the bulk oxide as to the tendency to form a crystalline structure. The surfaces of crystalline oxides also have unsatisfied bonds such as metal atoms on the free metallic surface. The attractive forces of the free oxide bonds are somewhat stronger for asymmetric molecules (such as water vapor) than for symmetrical molecules such as oxygen.

Thus, ordinary metallic surfaces are characterized by three features which prevent the formation of true metallurgical bonds, i.e., (1) adhered moisture layer, (2) the oxide film, and (3) atomic roughness. These features prevent intimate contact between atoms having incomplete molecular shells. The formation of a bond requires the removal of the surface films and smoothing out of the surface irregularities so that a large area of intimate metal contact is attained. The ultrasonic welding technique achieves just that. The metal surfaces are deformed under the action of the compressive force which breaks and disperses the oxide layer. The application of ultrasonic energy then softens the wire which allows it to further deform thus placing the materials in the intimate contact necessary for linking of the unsatisfied atomic bonds.¹

¹ All references are given in Section 6.

Gold and aluminum are the most common metal combinations used in micro-electronic assemblies. While aluminum is the usual element for metallization of semiconductor components, gold is the most suitable for metallization of ceramic substrates - either by thin film or by thick film processes. Interconnections are normally done by ultrasonic bonding of aluminum wire. It is thus necessary to consider the metallurgy of the gold-aluminum system when these metals are subjected to the process of ultrasonic bonding.

The literature lists five phases for aluminum-gold alloys, i.e., AuAl_2 , AuAl , Au_2Al , Au_5Al_2 , and Au_4Al . There has been disagreement on which of these phases is present in the aluminum-gold bond, on the kinetics of formation of each individual phase, on the contribution of silicon to the formation of these phases, and how these phases affect the strength of the aluminum wire bonds. Whatever the exact mechanism, the fact is that in some cases the gold-aluminum bond shows degradation in mechanical strength after prolonged exposure to high temperatures.

This program was undertaken to study and evaluate ultrasonic bonds of aluminum wire to ceramic substrates metallized with thin and thick film gold as well as wire bonds between such substrates and semiconductor chips. The bondability of thin film aluminum substrate metallization was also investigated.

The planning of the program, and the bulk of the investigation (including the bonding and pull testing on the thin and thick film gold substrates) was carried out by Milo Macha. The testing of the substrates with semiconductor chips, the bonding and testing related to the aluminum film, and the compilation of this report were performed by R. A. Thiel.

2. APPROACH

The basic experimental approach in this program has been:

- a. Establish a desired combination of materials and parameters to be investigated.
- b. Determine a bonding schedule for this combination.
- c. Bond the pattern for electrical measurements and measure the initial resistance.
- d. Perform the bonding for pull testing.
- e. Perform the initial pull testing. Bond strength was determined by MIL-STD-883, Method 2011, Test Condition "D". The observed pull strength as well as the mode of failure (wire break at heel of bond, separation of bond from substrate, or film failure) was recorded. On the specimens with semiconductor chips, the location of the failure (substrate or chip) was also recorded.
- f. Heat soak the substrates at 150°C for 72 hours and pull test. The heat soak is according to MIL-STD-883, Method 1008, Condition "C".
- g. Thermal cycle the substrates for 10, 20, 60, or 100 cycles from -65°C to +150°C and pull test. This is a modification of MIL-STD-883, Method 1010, Test Condition "C" involving additional number of cycles and the use of a thermal shock chamber which performs the transition between the temperatures in about 2 seconds compared to the 5 minutes allowed.
- h. Measure final electrical resistance.

2.1 SUBSTRATE AND WIRING PATTERN

The pattern of bonding pads shown in Figure 2-1 was employed for the whole study. The wiring pattern shown in Figure 2-2 was used for both the thick and thin film gold. This pattern accomplishes several requirements. It provides a large number of bonds in series (99 loops - 198 bonds) for the purpose of electrical measurements. In addition, it provides sites for a large number of bonds (50 loops - 100 bonds) of three different wire sizes on the same substrate. In these tests, the substrates were arranged in three groups. Group "A" had 25.4 μm (1 mil) series connections with 25.4, 38.1 (1.5 mil) and 50.8 μm (2 mil) jumper wires for pull testing. Group "B" had 38.1 μm series connections and three sizes of jumpers, and Group "C" had 50.8 μm series connections and three sizes of jumpers. From 30 to 37 substrates were used for each group and each type of metallization. Each substrate carried its own serial number for identification.

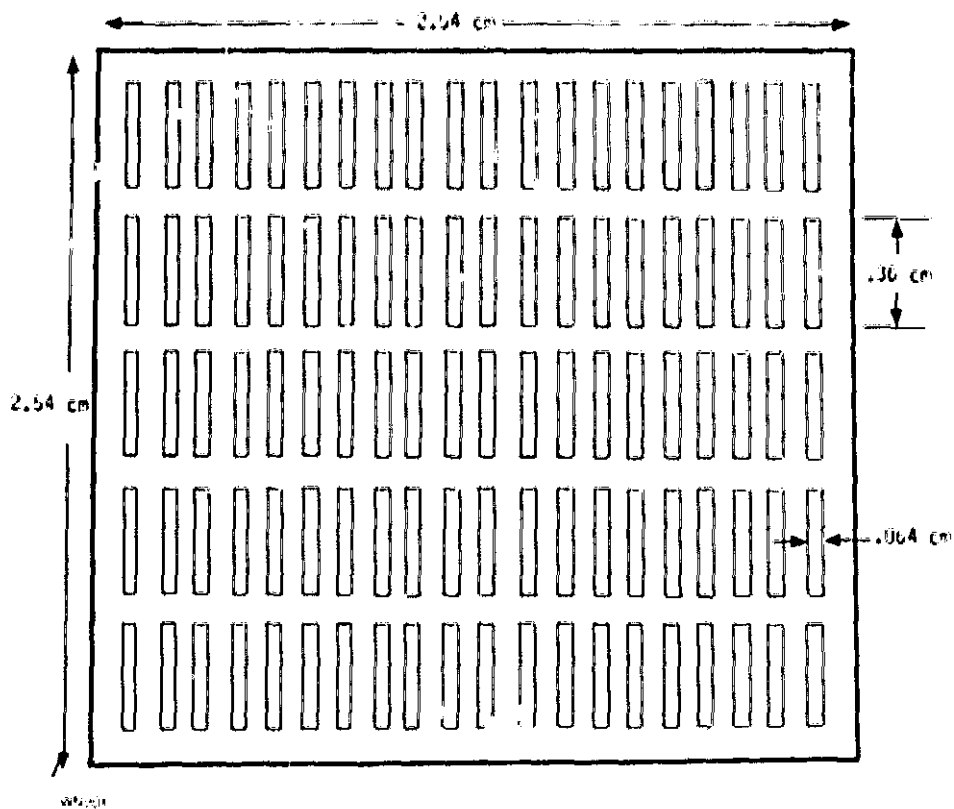


Figure 2-1. Substrate Pad Pattern

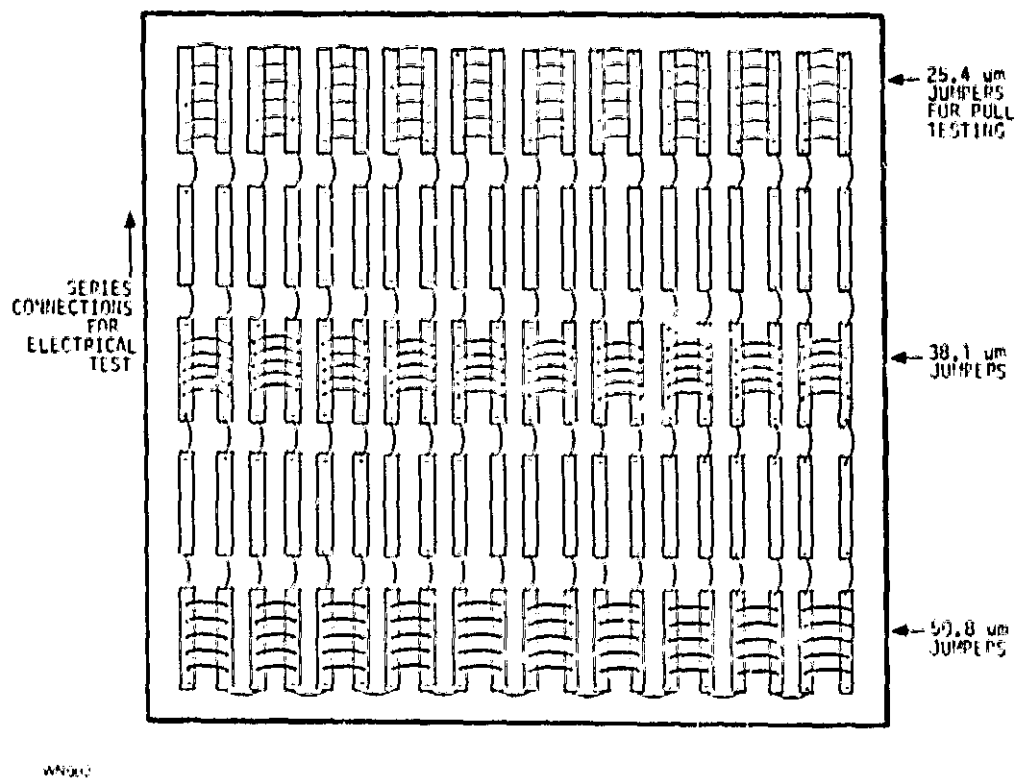


Figure 2-2. Wire Bond Test Pattern, Thick and Thin Film Gold

For the phase of the program involving semiconductor chips, ten chips were bonded to the substrate in a symmetrical array. About 30 wire bond loops were made for each substrate and a total of 100 substrates were made (25 each for 25.4 and 38.1 μ m wire and thick and thin film gold).

The exploratory testing on the aluminum was done in a somewhat different manner. The wiring pattern used here is illustrated in Figure 2-3. A single size wire was used on a given substrate. Two short sections of series bonds (9 loops - two groups/substrate) were made on pads not used for pull testing. All five columns were used for pull test jumpers. The bonds were kept away from the periphery of the substrate to eliminate some handling damage that had been experienced with the gold specimens. A total of 840 bonds were made and tested on five substrates.

In all, a total of more than 100,000 bonds were made for test purposes.

2.2 MATERIALS

2.2.1 THICK FILM GOLD

The substrates used for these specimens were 96% alumina (ALSIMAG 614) with an as-fired surface finish of $<.64 \mu$ m (25 μ in). The gold ink used was Electro-Science Laboratories #8835, a fritted gold, considered a representative ink employed in this technology.

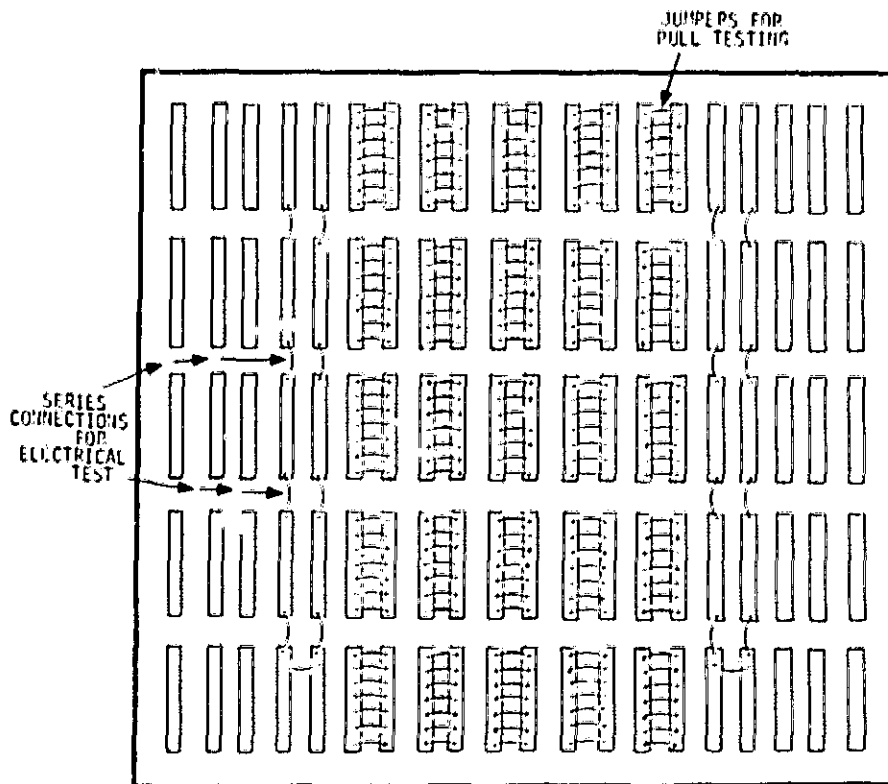


Figure 2-3. Wire Bond Test Pattern, Thin Film Aluminum

2.2.2 THIN FILM GOLD

The basic substrates here were 5.08 x 5.08 x 0.064 cm (2" x 2" x 0.025"), 99.5% alumina (Coors ADS 995), with an as-fired surface finish of $<0.25 \mu\text{m}$ (10 μin). The thin film metallization was produced by a standard process consisting of a flash evaporation of 60/40 Ni/Cr to a nominal thickness corresponding to 200 Ω/square , followed by 1000 Å of 99.99% gold, also by flash evaporation. After removal from the vacuum system, the gold thickness was built up to 2.5 μm (100 μin) using an acid gold plating bath (Englehard E56). After etching a 2 x 2 stepped array of the standard pattern into the metal, the substrates were sawed into the standard 2.54 x 2.54 cm specimen format.

2.2.3 THIN FILM ALUMINUM

This material was deposited by flash evaporation to a thickness of 1.6 μm on 5.08 cm square, 99.5% alumina substrates, which after etching were sawed to the standard size.

2.2.4 BONDING WIRE

The aluminum wire used was UBG grade, 1% Si-Al from Secon Metals Corp. The specifications on the three sizes of wire as received are listed in Table 2-1.

2.2.5 SEMICONDUCTOR COMPONENTS

Silicon transistor and IC chips were obtained from Motorola, Raytheon, Texas Instruments, and Fairchild. They were attached to the substrates in a symmetrical array using epotek H-41 (epoxy technology inc.) a single component gold filled epoxy.

2.3 EQUIPMENT

The majority of the equipment used to produce the substrate metallization pattern consists of standard off-the-shelf units of types commonly found in the industry (outside of occasional identification, little further information about them will be given). However, some equipment or equipment problems are of special interest and will be discussed in some detail.

Table 2-1. 1% Si-Al Wire

DIAMETER [μm (mils)]	ELONGATION (%)	TENSILE STRENGTH (gmf)
25.4 (1)	1 to 3.5	14 to 16
38.1 (1.5)	2	20
50.8 (2)	3.1	76

2.3.1 VACUUM EVAPORATOR

The vacuum evaporator used to deposit the thin film gold and aluminum is an in-house design which has evolved over the years into a unique and versatile tool. It is shown in Figure 2-4. Its design is based on the combined merits of flash evaporation and planetary motion of the substrates. The flash evaporation is accomplished by feeding a wire of the material to be evaporated onto a resistance heated tungsten strip, 1.27 cm wide x 0.508 mm thick (0.5" x 0.020") held between two chucks 4.44 cm (1.75") apart. When the wire contacts the strip, it melts and quickly evaporates, resulting in a series of small vapor pulses. Since effectively, a very large number of very small charges are each evaporated to completion, fractionation of alloys is eliminated.

The technique can in principle be used for any material available in wire form which can be melted and evaporated from a suitable resistance heated boat. It has been used to deposit 80/20, 70/30, 40/60 and 30/70 Ni/Cr alloys, 80/20 Ni/Fe, gold, copper, nickel and aluminum. Large amounts of nickel and aluminum are difficult to deposit by this technique since both materials attack the hot tungsten strip and ultimately cause it to break. However, with the present geometry typically 5000 Å of either material can be deposited before the tungsten fails. Thus, with the small amount of Ni/Cr required (≈ 175 Å) for a 200 Ω /square resistive film no problems are experienced in normal deposition of Ni/Cr - Au films for thin film hybrids. Several materials such as Ni/Cr and gold are easily deposited in sequence by simply welding the required lengths of the different materials in series to make a single wire. Furthermore, no monitoring of the deposited film is necessary for control purposes since a simple measurement of wire mass or length quite adequately determines the amount of film deposited, and the voltage to the dc wire feed motor in conjunction with the wire diameter accurately controls the deposition rate. A barrier layer of up to about 4000 Å of Ni can also be deposited by the same method. Normally 30 mg of 40/60 Ni/Cr wire followed by 10.16 cm (4") of 0.0508 cm (20 mil) dia. Au wire produces a 200 Ω /square resistive film covered by about 1000 Å of Au.

For the deposition of the 1.6 μ m Al films, the Al wire was fed until the source failed, the substrates were allowed to cool, the system opened, the tungsten strip replaced and the whole sequence was again repeated twice more. A preliminary investigation has revealed that it should be possible to substitute a boron nitride-titanium diboride boat for the tungsten strip, using the same power supply. This composite material has been used successfully by the metallizing industry to deposit large amounts of aluminum, the only difference being that since fractionation is not a problem, the source is run slightly cooler and a puddle is allowed to form in a depression milled in the top surface of the boat.

The substrate holding system (shown in Figure 2-5) consists of four 11.43 x 11.43 cm (4.5" x 4.5") flat planets. Each planet includes a radiant substrate heater located 1.27 cm (0.5") behind the substrates. Typically, the substrates are heated to a peak temperature of 360°C, after which the substrate heaters are shut off and the substrates allowed to cool to about 300°C before deposition begins. Substrates of various sizes are held in the planet by



Figure 2-4. Vacuum Evaporator

ORIGINAL PAGE IS
OF POOR QUALITY

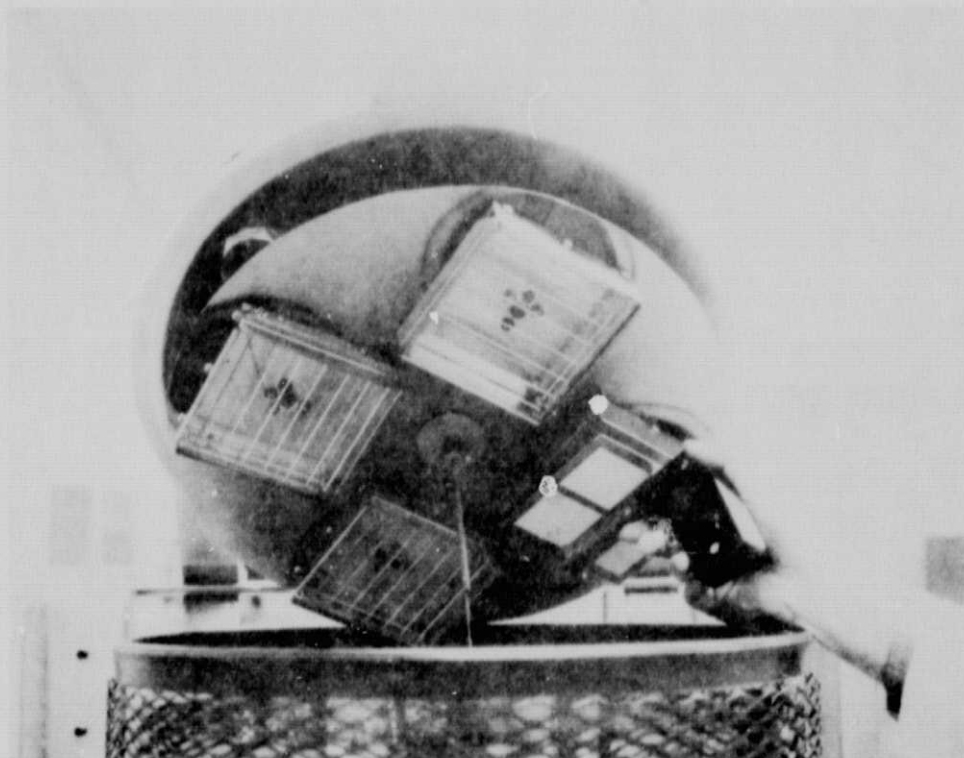


Figure 2-5. Loading Vacuum Evaporator

removable window frames having appropriately sized holes. Four of the standard 5.08 x 5.08 cm substrates are accommodated by a single planet, for a total of 16 substrates per deposition. The height of the source is set to maximize the uniformity of the Ni/Cr films.

The pumping module consists of a 2000 liter/second oil diffusion pump using DC 705 oil, isolated from the chamber with a water cooled chevron baffle, an LN₂ cooled chevron baffle and a gate valve, and backed by a 500 l/sec mechanical pump.

2.3.2 BONDER AND ULTRASONIC POWER SUPPLY

The bonder used, a K&S Model 484 with a UTI Model 10C-7 ultrasonic power supply is shown in Figure 2-6. This equipment is widely used in the industry. Properly adjusted it can produce consistent bonds. However, careful machine setup and monitoring are required to avoid equipment related problems. Some of the potential problems with this bonder which have been reported are vibration problems² and timing of the ultrasonic pulse relative to bonding tool force³. We have observed a different problem which may occur intermittently. (This machine behavior was observed on a bonder never actually used to make bonds for this study.)

The problem first presented itself as an occasional failure of the bonder to halt at the RESET point after the second bond. The machine would complete the second bond, pull the wire, continue through the RESET position and finally stop at the 1st SEARCH position. The

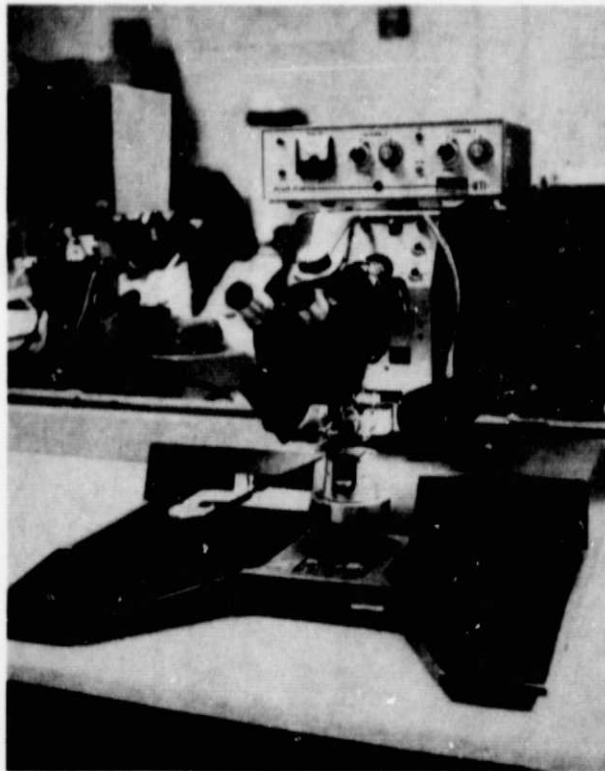


Figure 2-6. Ultrasonic Bonder

behavior was very erratic, occurring several times on some days and never on others. After several unsuccessful attempts at rectifying the fault (all aimed at correcting an assumed erratic contact in the operator's control switch) it was discovered that a more subtle fault was also occurring. This fault consisted of an occasional double application of the ultrasonic power to the first bond. This fault was never noticed by the operator, but was discovered only as a result of responding to her complaints about the RESET overrun. It was first noticed as an occasional "different" rhythm during the first bond sequence. It was further characterized as a sort of hesitation. After the fault was noticed, it was also observed that the resulting bond was more squashed than normal. The fault seldom occurred on the same cycle as a RESET overrun.

This bonder uses mechanical cams and a photoelectric shutter system on the same shaft to coordinate the various mechanical and electrical operations. The photoelectric shutter consists of a circular disc with holes located to allow light to reach the photocells at the appropriate times in the cycle. Although the RESET stop and the LOOP stop are controlled by the same cell, no overrun of the LOOP position ever occurred. Likewise, the ultrasonic generator is triggered for the 1st and 2nd bonds by another cell, but no problem ever occurred on the 2nd bond. Dirt in the shutter holes was eliminated as the cause, as well as malfunction of the lamp-photocell combinations.

Control of the cam motor rotation is derived from three sources: the operator's switch which provides starting signals; two of the photoelectric cells which provide stop signals; and the ultrasonic generator which stops the motor at the beginning of the ultrasonic pulse, and re-starts it at the end of the pulse. The ultrasonic generator is itself triggered by signal from a third photocell.

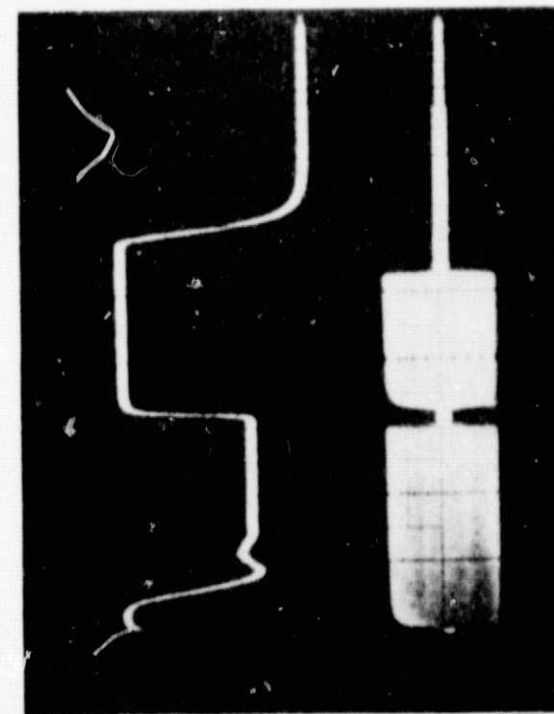
A storage scope was used to track down the problem. Figure 2-7A shows a normal signal from the trigger photocell as the upper trace and the resulting ultrasonic pulse (set extra long at 300 μ s for illustrative purposes) as the lower trace. In all pictures following, the horizontal time scale is 100 ms/division, and a high level signal from the photocell indicates that its shutter is open. The sequence of events is as follows. As the shutter opens, the rising level is differentiated at the input of the generator and used to trigger the timed ultrasonic pulse. Simultaneously, the motor which turns the cam is shut off. At the end of the ultrasonic pulse, the motor is again turned on, and as the cam moves, the shutter closes. Figure 2-7B shows what happens when a double pulse occurs. In this case, after triggering the ultrasonics and stopping the motor, the cam rolls backward, which at least partially re-closes the shutter. When the ultrasonic pulse is complete, the motor re-starts, which re-opens the shutter, causing the generator to be re-triggered and the motor to stop again. Some maximum amount of rollback (as illustrated in Figure 2-7C) can be tolerated and will not cause re-triggering. On any given cycle, any one of the conditions illustrated could occur, resulting in erratic operation.

TRIGGER SIGNAL

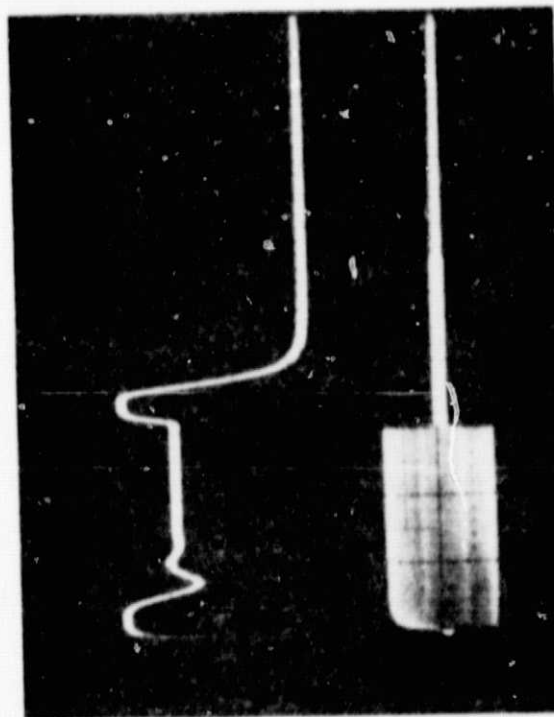
ULTRASONIC PULSE

.1 SEC →

(A) PROPER OPERATION



(B) DOUBLE FIRING



(C) TOLERABLE ROLLBACK

Figure 2-7. First Bond Problem

WN007

A similar kind of problem occurs at the RESET position. The pictures in Figure 2-8 show the generator trigger signal as the upper trace and the photocell stop signal as the lower one. Figure 2-8A illustrates a normal condition: here, the trigger signal of a 1st bond followed by the stop signal at the LOOP position.

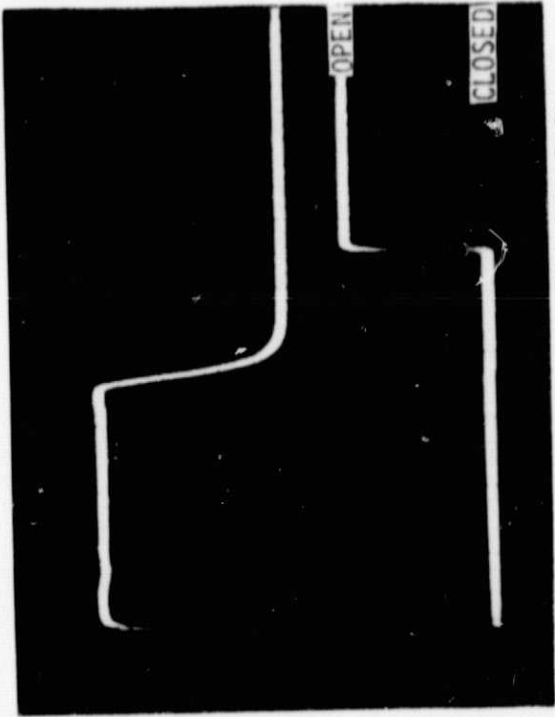
Figure 2-8B shows the trigger signal of a short 2nd bond and the following stop signal at the RESET position. What happens is that when the shutter opens, the motor stops. But then the cam rolls so far backward that the shutter re-closes and the motor re-starts, again opening the shutter - which stayed open this time. Figure 2-8C shows a similar case. But this time after re-starting and again stopping, the cam rolled too far forward and the hole in the shutter almost overshot the photocell. If it had gone just a little farther, the motor would have again re-started, resulting in an overshoot RESET. On the day these pictures were made, although the motor frequently re-started once at RESET, it would not completely overshoot.

New models of the 484 are equipped with a dc cam drive motor rather than the stepping motor on this unit (reportedly because it results in more precise stopping; it should also produce less vibration). By adjusting the phasing of the photocells relative to the mechanical cam followers, it was possible to almost eliminate both problems. However, this bonder is being retrofitted with a dc motor.

In the process of making the phase adjustment, an additional problem similar to one observed by Un... was noted³. He reported receiving new machines adjusted in such a manner that the ultrasonic pulse occurred before the force of the ultrasonic bonding tool on the wire/pad interface had stabilized. The machine lowers the tool by lowering a support which effectively holds the tool up. When the tool contacts the substrate, the support continues downward. The distance the support drops from the SEARCH position to its lowest point is fixed by a mechanical cam. The time of firing of the generator is determined by the relative phasing of the cam follower and the photocell. Figure 2-9 illustrates the operation, with a, b, and c indicating possible points at which the photocell could be adjusted to fire the generator. If triggering occurred at a, with the search height as shown, the tool and wire would just barely make contact with the substrate when the generator fired. Later triggering at b, or even c, would assure that the force had stabilized before the ultrasonics began.

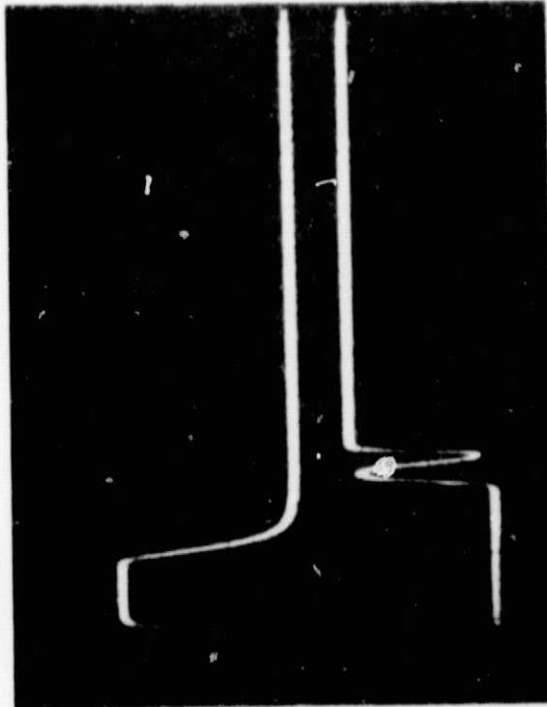
During the phase adjustment, it was discovered that the previous setting corresponded to a location on the descending slope similar to the point marked a. Such adjustment could make bonding very sensitive to search height adjustment. At first look, the search height adjustment is set adequately low if overtravel of the support is observed during the cycle; but firing on the descending slope could easily invalidate such a conclusion. This problem could be particularly troublesome when working with hybrids in which chip heights may typically vary by several wire diameters. The usual technique is to set the search height to clear the highest chip and then use the Z-lever to individually readjust the actual search to a lower value for accurate targeting. When bonding to large pads, an operator could conceivably fail to lower the search enough and could get a poor bond due to premature firing even though overtravel occurred.

TRIGGER SIGNAL

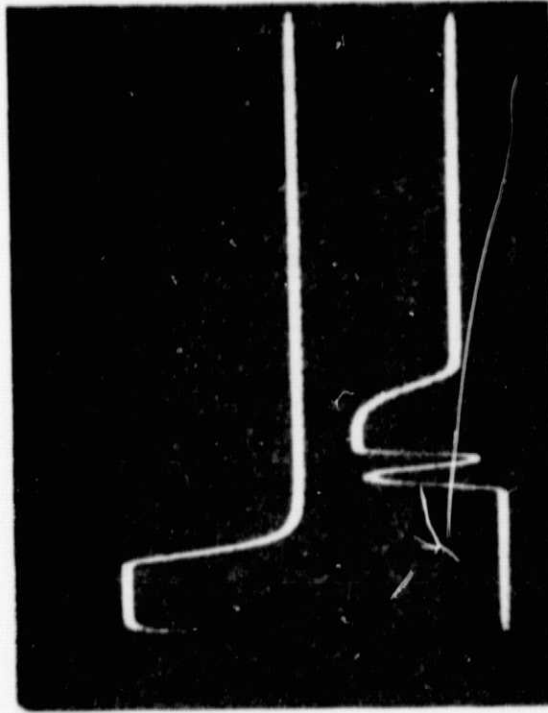


STOP SIGNAL

(A) PROPER STOP AT "LOOP" POSITION



(B) STOP & RESTART AT "RESET" POSITION

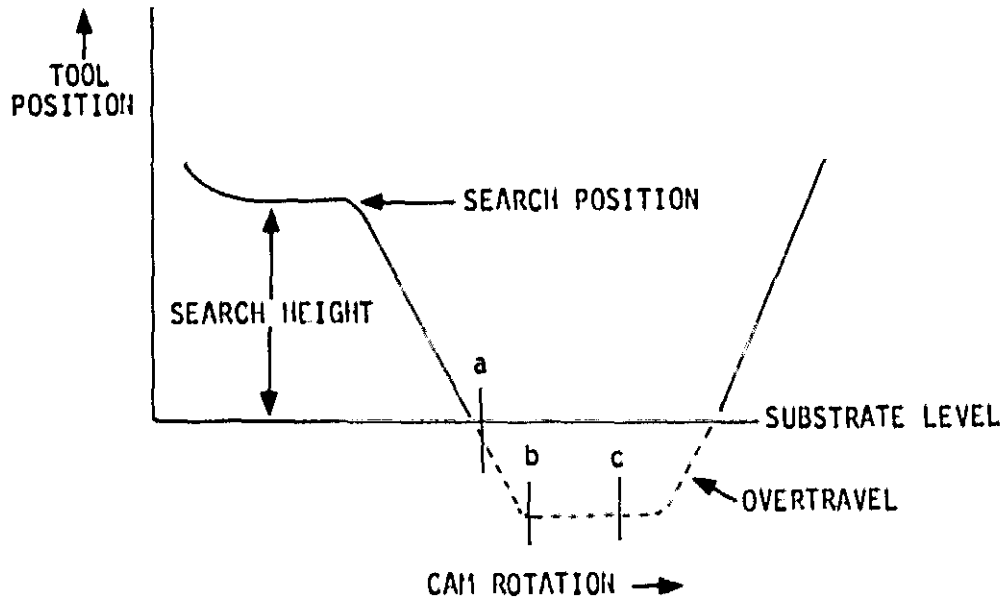


(C) NEAR OVERSHOOT AT "RESET"

ORIGINAL PAGE IS
OF POOR QUALITY

WN008

Figure 2-8. Reset Problem



WN009

Figure 2-9. Bonder Timing

2.3.3 BONDING TOOLS

The tungsten carbide bonding tools used in this program were obtained from the Gaiser Tool Co. Their characteristics are listed in Table 2-2.

Late in the program we began using a new method of cleaning the tool as suggested by Unger⁴. The method consists of placing a piece of unfired alumina in the bonder work holder, pulling back the wire from under the foot of the tool and repeatedly cycling through the bonding sequence. The initial sequences leave a dark residue of aluminum on the white surface of the plastic-like alumina. When the tool is clean, the impression of the tool is seen in the alumina, but without any discoloration. After rethreading the tool and making a few bonds to "recondition" the surface of the foot, the tool is again ready for routine bonding. This method has several advantages. Besides the obvious temporal advantage of not having to remove, clean and replace the tool in the machine, it has been well established by G. Harman et al. of NBS⁵ that even loosening and re-tightening the screw which holds the tool requires re-calibration of the bonder. We have not thoroughly evaluated this method over a long period of time, but it cleans the tool very effectively, and we have seen no evidence of any disadvantages.

Table 2-2. Ultrasonic Bonding Tools

P/N	HOLE DIA. μm (mils) $\pm 5 \mu\text{m}$	BOND LENGTH μm (mils) $\pm 5 \mu\text{m}$	MAX. CONCAVITY μm (mils)	BACK RADIUS μm (mils)
2012-20L	50 (2)	64 (2.5)	8 (0.3)	8 (0.3) Contoured
2013-20L	50 (2)	76 (3)	8 (0.3)	- Contoured
2022-25L	64 (2.5)	76 (3)	8 (0.3)	- Contoured
2023-35L	89 (3.5)	76 (3)	10 (0.4)	- Contoured
2024-35L	89 (3.5)	101 (4)	10 (0.4)	- Contoured

2.3.4 BONDING TOOL INSPECTION FIXTURE

Occasionally a particular bonding tool was observed to scrape the wire. In other cases, certain repeating abnormal deformations of the bond suggest that some defect exists in the foot of the tool. After considerable difficulty was experienced trying to inspect tools under a microscope, an inspection fixture designed. This fixture is shown in Figure 2-10 on the stage of a measuring microscope which can also be used to critically measure the tool dimensions. The fixture allows the tool to be rotated about two axes. The tool is located in the fixture using a positioning gage which ensures that the two axes of rotation intersect at the surface of the foot. In this way, the whole foot can be examined from any angle at 30x or 100x with a minimum of re-focusing. Oblique lighting has been found to be superior for this kind of inspection. Bottom light through the transparent glass stage enables the hole in the tool to be inspected.

2.3.5 THERMAL CYCLING CHAMBER

A Blue M, Model WSP 109C-3 Dual Thermal Shock Test Cabinet (shown in Figure 2-11) was used for the thermal cycling tests. The work to be cycled is placed on a low mass elevator having a suitably insulated floor and ceiling. The elevator periodically cycles the work between the upper heated chamber and the lower cooled chamber, with the transition being made in about two seconds. Blowers circulate the air in both chambers. This unit although it works adequately, has several undesirable features which could be improved.

The timer used to control the transfer from hot to cold and vice versa is adjustable from 0 to 5 hours and is poorly calibrated at short times. The cycle time used for this program and for testing typical microcircuits calls for 10 minutes at each temperature. Thus achieving a reasonably accurate 10-minute half cycle requires a considerable amount of time consuming trial and error.

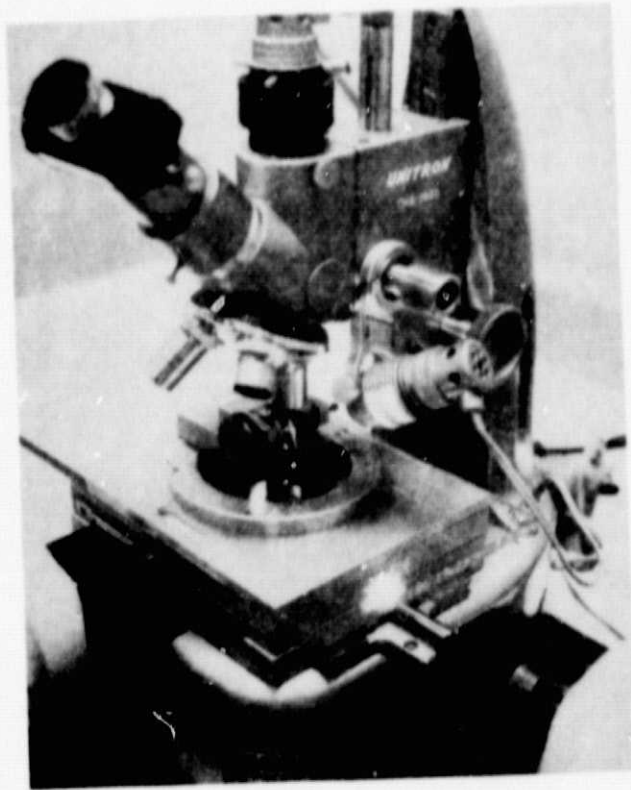


Figure 2-10. Tool Inspection Fixture



Figure 2-11. Thermal Shock Chamber

A high quality controller is used for the low temperature chamber, but it also has a poorly chosen range (-100°C to $+300^{\circ}\text{C}$). Since there is no provision to heat this chamber and room temperature is at less than 25% of the physical length of the scale, 75% of the scale can never be used, and setting the instrument to within $\pm 5^{\circ}\text{C}$ at -65°C is very critical. Careful calibration has established the excellent accuracy of the control, but its ability to be set accurately leaves much to be desired.

The elevator mechanism exhibits a destructive lateral jerk at its two extremes. As a result, a batch of 100 substrates which were packaged for this test in glass petri dishes received extensive damage when the substrates within the dishes (four per dish) shifted laterally and ended up on top of each other. The only safe packaging scheme for unprotected samples in this chamber is in individual dishes.

2.3.6 OTHER EQUIPMENT

A Mech-E1 Model BT-202 wire bond pull tester shown in Figure 2-12 was used for the majority of this investigation. The unit employs a conventional gram force gage, which is rotated about the axis of the lever arm by a small motor. A vacuum chuck holds the substrate. An adjustable upper limit switch enables the unit to be used as a non-destructive tester if desired.

A force gage fixture shown in Figure 2-13 was designed along the lines recommended by NBS⁶ in order to more accurately set and monitor the bonding force exerted by the tool on the bond interface during bonding. Also shown in the figure is a torque wrench used to repeatably tighten the set screw which holds the bonding tool in the transducer horn.

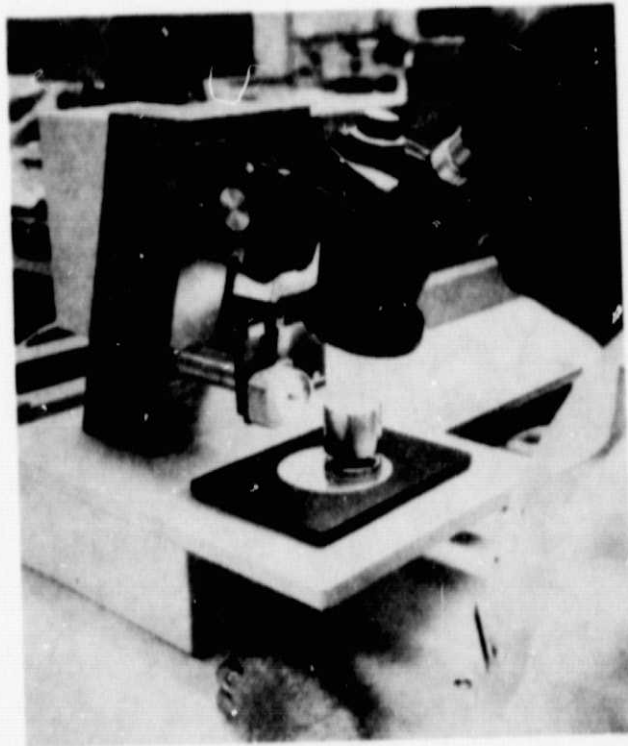


Figure 2-12. Wire Bond Pull Tester

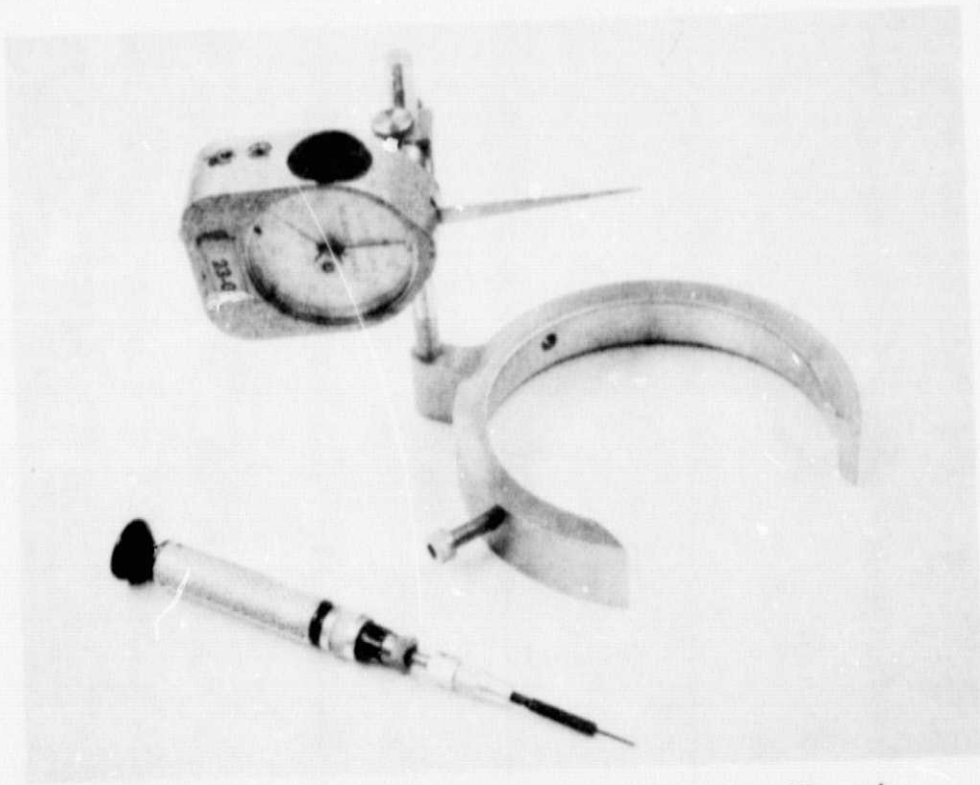


Figure 2-13. Bonding Force Gage and Torque Wrench

2.4 PROCESSES

2.4.1 THICK FILM GOLD SUBSTRATES

The bonding pattern (Figure 2-1) was printed on 200 mesh stainless steel screen using a 25- μ m thick D-Cote emulsion. After the gold pattern was screened on the substrates, it was dried and fired in a seven-zone BTU belt furnace at a peak temperature of 882°C with the temperature held above 875°C for 10 minutes. The air flow through the furnace was 12 atm-liter/min. The as-fired gold was 10-12.5 μ m thick with a surface finish of 0.5 μ m as measured on the Talysurf. The overall process of fabrication and testing is shown in Figure 2-14.

2.4.2 THIN FILM GOLD SUBSTRATES

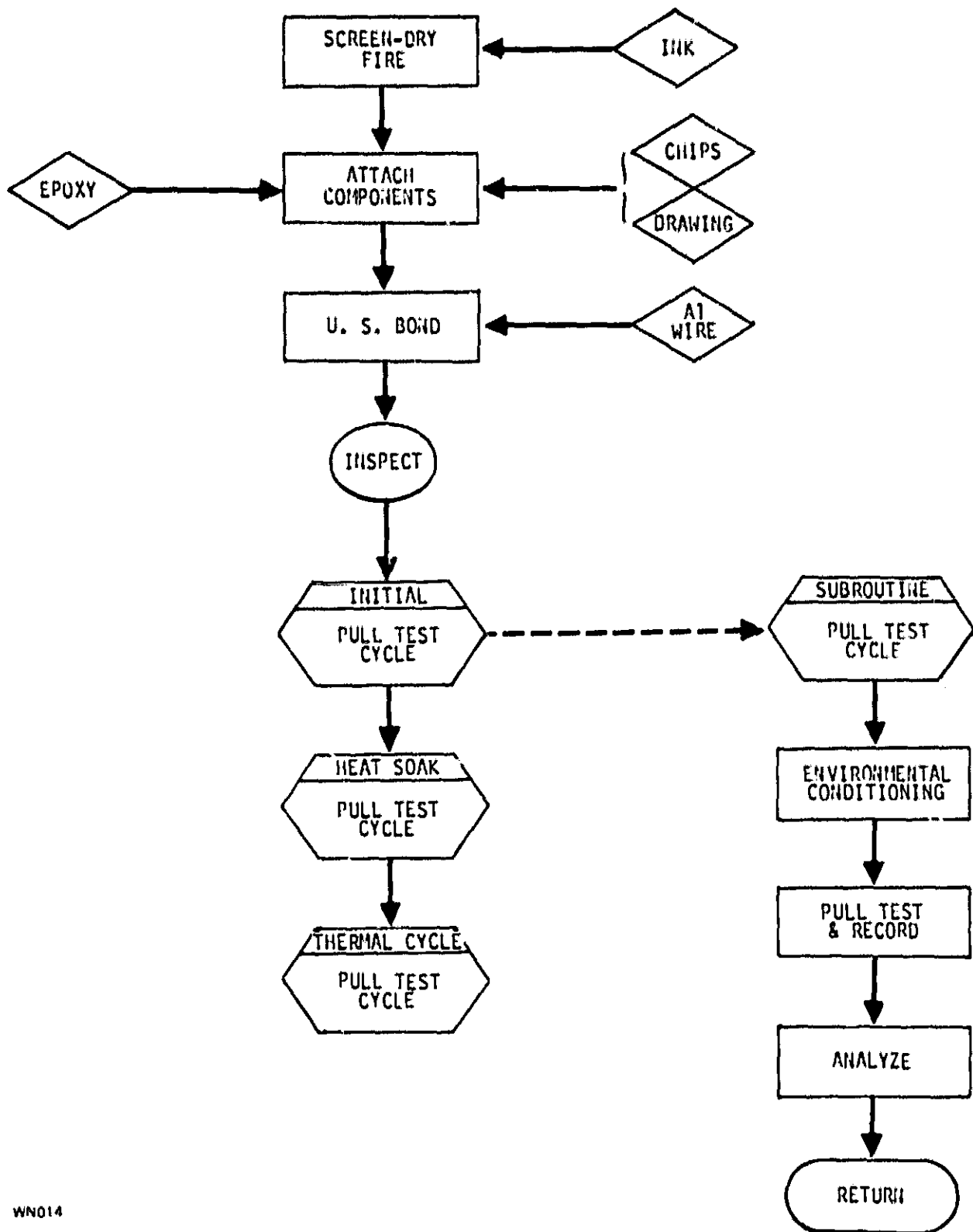
The following processes which were used to make the thin film substrates are standard processes and are documented by manufacturing specifications.

The cleaning procedure for the substrates consists of the following:

- a. 15-minute ultrasonic agitation at 66°C in Alconox solution.
- b. 10-minute rinse with ultrasonics in running DI water.
- c. 20-minute soak in solution of 1 part (by volume) DI water, 1 part 58% ammonium hydroxide and 2 parts 35% hydrogen peroxide.
- d. 5-minute rinse with ultrasonics in running DI water.
- e. Immersion in five-tank cascade DI water rinser at 60°C; 2 minutes in each of the first four tanks, 5 minutes in the last one.
- f. Cool in DI water.
- g. Dry in isopropyl alcohol vapor.

The cleaning is completed in a laminar flow clean bench where the substrates are loaded into the evaporator window frames and carried to the evaporator in a clean stainless steel can. The whole process is arranged so that the "good sides" of the substrates are either vertical or facing downward until after the deposition is complete. The window frames are removed from the carrier and placed in the evaporator using a gun-like tool which eliminates direct contact with the frames or the planets by the operator. See again Figure 2-5. This method virtually eliminates particulate and handling contamination.

The major details of the evaporation process have already been covered in the description of the vacuum system. Normally the Ni/Cr film is used as the resistive layer in the thin film hybrid, and as the adhesive layer for the gold film. But for this study, it merely serves the latter purpose.



WN014

Figure 2-14. Ultrasonic Bond Study, Thick Film Flow Chart

After deposition, the substrates are electroplated at a current density of .36 amp/dm² in an acid plating bath (Englehard E-56) held at 60± 2°C. This operation produces the actual bonding surface.

The photolithographic process uses Shipley 1350J, which is filtered at the time of application. The mask is a stepped 2 x 2 array of the bonding pattern. Etching is accomplished using Techni-Strip Au and Transene TFC for the gold and Ni/Cr respectively. In the normal hybrid process, a re-exposure with the resistor mask and a second gold etch defines the resistors at this point, but that operation was unnecessary here. The resist is stripped with acetone, after which the substrates are sawed into 2.54 x 2.54 cm squares. The overall process flow chart is shown in Figure 2-15.

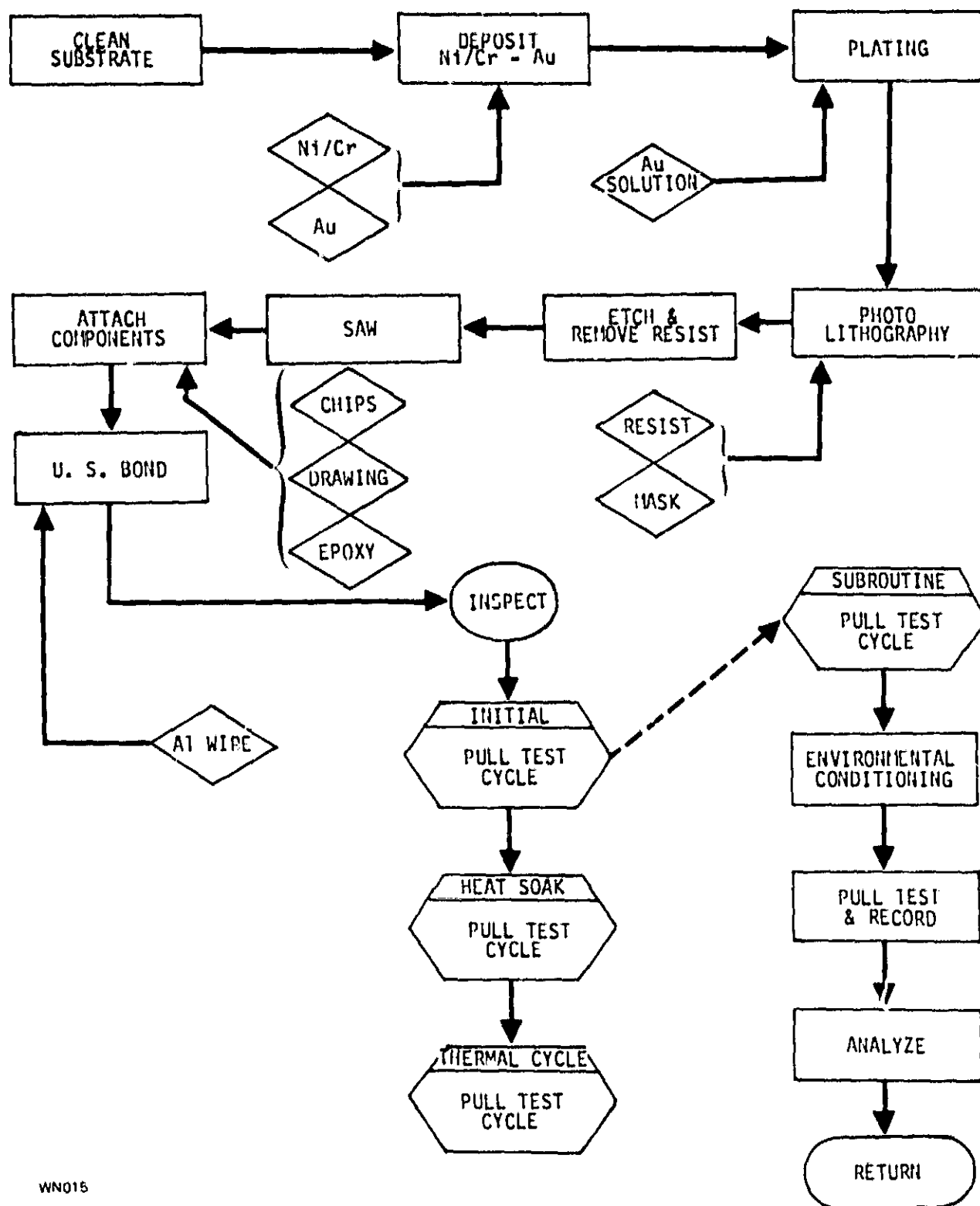
2.4.3 THIN FILM ALUMINUM SUBSTRATES

The standard cleaning procedure was used, followed by the deposition sequence already described in the equipment section. The same photolithographic methods were employed except that the etchant was 80 parts (by volume) concentrated phosphoric acid and 5 parts concentrated nitric acid. The substrates were separated by sawing. The overall process is shown in Figure 2-16.

2.5 DATA ANALYSIS

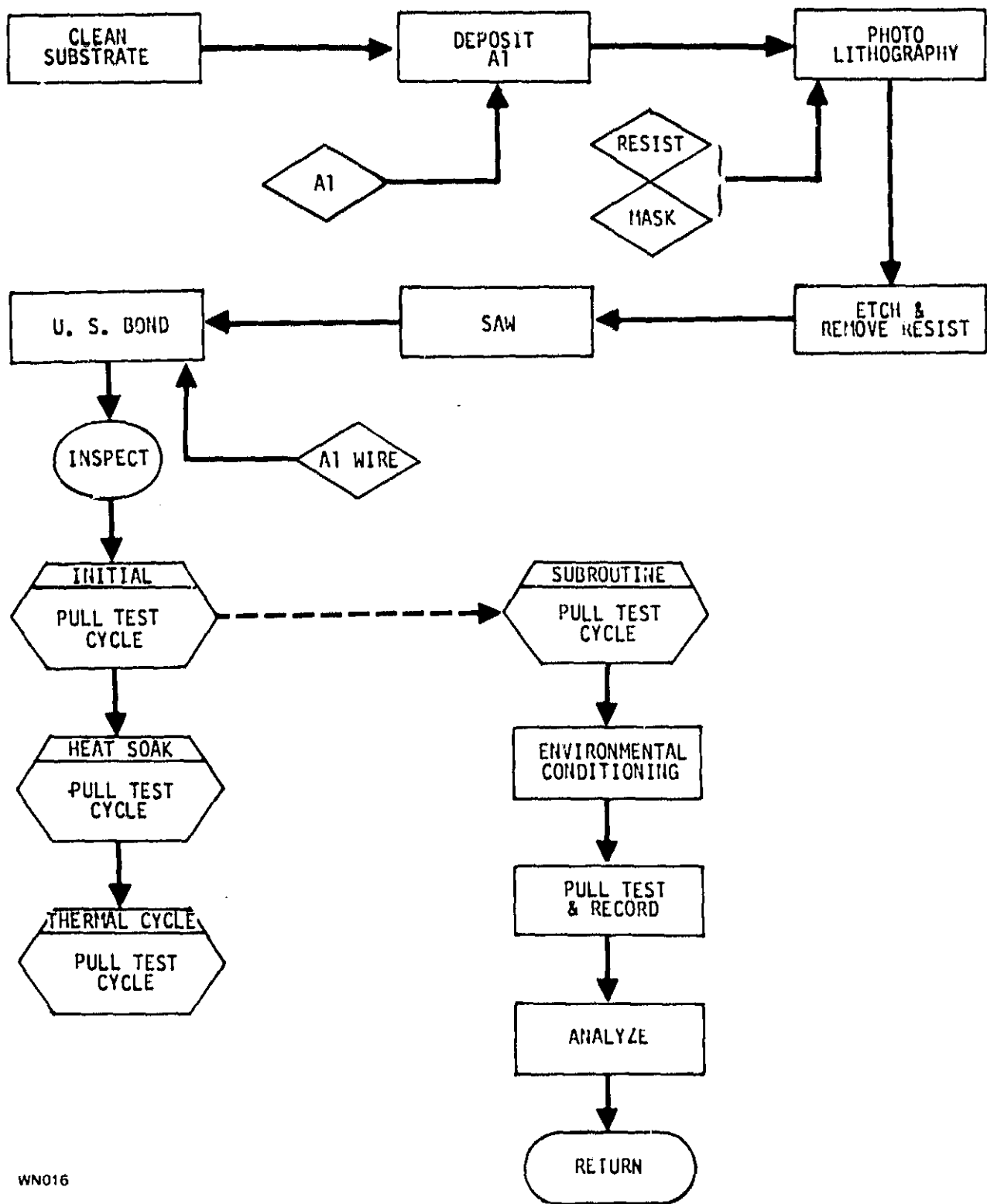
During the pull testing operation, each pull strength was recorded as well as the failure mode (break of the wire at the heel of a bond, separation of wire from the metallization, or film failure). On the specimens involving chips, the location of the break was also recorded. Typically, 10 bonds were pulled per substrate for each test category, and a separate data sheet was kept and identified for each substrate. For data analysis, a program was written for the HP 9100B calculator.

Figure 2-17 describes the printer output. Shown is the end of a calculator tape resulting from a batch of substrates numbered 8 through 34. The reason for printing out the cumulative sums is to allow the operator to re-check the data from a given substrate without having to start again from the very beginning. The program has a simple provision for resetting these cumulative sums to any desired values in case an error is made. When data from all substrates in a batch has been entered the second section of the program is entered which prints out the three sums, the overall mean, the standard deviation, and the % standard deviation.



WN015

Figure 2-15. Ultrasonic Bonding Study, Thin Film Flow Chart



WN016

Figure 2-16. Ultrasonic Bonding Study, Al Thin Film Flow Chart

3. DATA

3.1 THICK FILM ONLY

The data from the thick film samples is summarized in Tables 3-1, 3-2, and 3-3 for the 25.4 μm , 38.1 μm and the 50.8 μm wire respectively. (All the tables appear at the end of this section.) The bonds with 25.4 μm wire in Group A were all made using a bonding tool which produced a 64 μm bond length, whereas those in Groups B and C had a 76 μm bond length. All 38.1 μm wire bonds were made with a 76 μm bond length, and the 50.8 μm bonds were made with a 101 μm bond length.

There was a general tendency for all the bonds made to thick-film gold to lose from 40 to 50% of their initial strength after the 72 hour heat soak at 150°C. Relatively little or no additional loss occurred after thermal cycling, even after 100 cycles.

During the initial pull testing, the mode of breaking was predominately at the heel of the bonds for the 25.4 and 38.1 μm wire, while for the 50.8 μm wire about 50% of the bonds broke at the heel and 50% peeled the film from the substrate. After heat soak, practically all of the 25.4 and 38.1 μm bonds separated at the interface between the wire and the film. The same mode was observed in about 50% of the cases for the 50.8 μm wire, while the other 50% still peeled up the film.

3.2 THICK FILM WITH CHIPS

A 76 μm bond length was used for both the 25.4 and the 38.1 μm wire. No bonds were made with the 50.8 μm wire because the bonding pads on the chips were not large enough to accommodate this wire size.

It became obvious during the pull testing that the geometry of the wire from chip to substrate was much less ideal from a measurement standpoint than the substrate to substrate wire geometry previously studied. Because of the particular substrate pattern used, wire lengths varied over a range of almost 3:1. Using the simplest possible resolution of forces calculation for a single level system and assuming a frictionless hook, such a variation in bond length could easily result in a 50% variation in the indicated pull strength for bonds of constant true strength. Thus, the chip data probably has more spread than the true case.

The pull test data is shown in Table 3-4. Pull strengths of ≤ 2 gmf for the 25.4 μm wires and of ≤ 4 gmf for the 38.1 μm wires are considered indication of a failed bond. Observed failures are listed separately and are not included in the averages. The specimens of both sizes received damage during the thermal cycling. Although the 25.4 μm samples received only minor damage, the 38.1 μm samples were extensively affected. In both cases, only wires which had not been disturbed were pulled.

The 25.4 μm data agrees with the 25.4 μm film-only data. However, the 38.1 μm pull strengths are significantly higher than in the film-only case. In addition, the reduction of strength after heat soak was only about 30% instead of the 40-50% shown in Table 3-2. 100 cycles of thermal cycling did not produce any significant additional change.

The bi-level nature of the film-chip geometry along with the friction forces on the wire at the hook result in a concentration of the applied force at the substrate bond. As a result, on the initial pull more than 80% of the breaks occurred at the first or substrate bond. The same pattern of predominately heel breaks on the initial test and bond separations after heat soak was repeated. In those cases in which the break occurred at the chip, the failure mode was either a bond separation or a combination of separation and film failure. After heat soak, virtually all breaks occurred at the substrate bond.

3.3 THIN FILM ONLY

The data for the thin film samples is summarized in Tables 3-5, 3-6, and 3-7. In Table 3-5, the 25.4 μm wires on the substrates in Group A1 had a 64 μm bond length. The use of the 76 μm bond length in Groups A2, B, and C resulted in substantial increase in bond strength, which was retained through heat soak and thermal cycling relative to the shorter bonds. All 38.1 μm bonds were made with a 76 μm bond length, and the 50.8 μm bonds were made with a 101 μm bond length.

There was a general — but in this case not universal — tendency for a reduction in pull strength after heat soak. In all cases however, the change was less than with the thick film. A difference in the failure mode was also noted. First, although the failure mode in the initial tests was predominantly due to heel breaks, some bond separations did occur, especially among the 38.1 μm samples. But after heat soak, contrary to the case with the thick film, virtually all breaks occurred at the bond heel. Film failure was not a problem with the 50.8 μm wire.

An anomaly occurred with the 38.1 μm wire. In two groups out of three, the pull strength increased after heat soak, but then dropped below the initial values after the temperature cycling. The overall change after cycling was only about 15% relative to the initial value, rather than the 30 to 40% typical of the 25.4 and 50.8 μm wire.

3.4 THIN FILM WITH CHIPS

A 76 μm bond length was used for both the 25.4 and the 38.1 μm wire. The test data are shown in Table 3-8. As with the thick film specimens, these also received damage during thermal cycling. The 38.1 μm specimens were virtually untouched, so a full-size sample of undisturbed wires was available for pulling. Unfortunately, the 25.4 μm samples were so extensively damaged that if only undisturbed wires had been pulled, the sample size would have been very small. Therefore, before the pulling began, the wires in this group were classified as undisturbed, moderately damaged, heavily damaged, very heavily damaged, or

hopeless. The very heavily damaged wires required some effort to get the hook under the wire, whereas the hopeless ones were so bad that no effort was even made. After pulling some of the wires, it was discovered that it was quite simple to mistake a wire which had been pulled up on a previous test and subsequently pushed back down on the substrate with a legitimate failure. Since true failures were indistinguishable, no failure information is given in the table.

Since what was to be the primary data from the undisturbed and moderately damaged classes was largely derived from wires whose strength might have been compromised by damage, the data from the heavily and very heavily damaged classes were also grouped together for analysis. Surprisingly, there is little difference between the two groups. This lends some justification to accepting the primary data as valid.

The 38.1 μm pull strength dropped about 15% after heat soak, and did not change after 100 thermal cycles. The 25.4 μm pull strength dropped about 30%, and also remained stable after temperature cycling. The failure mode of about 25% of the 25.4 μm bonds involved the chip end of the wire with almost all separating at the interface or separating with film failure. About 15% of the 38.1 μm bonds failed in the same way.

3.5 THIN FILM ALUMINUM

In experimenting with bonding to aluminum film on ceramic substrates, considerable effort was expended to control the wire geometry and to establish an optimum bonding schedule. The wire loop length was set by installing the appropriate step-back cam into the bonding machine, and the operator did not move the chessman between the first and second bonds. With this arrangement, excellent control is also maintained over the loop height.

The geometry terminology is defined in Figure 3-1. Loop height was determined with the depth gage on the measuring microscope (Figure 2-10) by focusing on the substrate, the highest point of the wire loop, measuring the difference with the dial gage and subtracting the wire diameter. The height was determined for the wire as bonded, and after the wire had been pulled (non-destructively) with a force of 8 gmf applied at mid span. If one assumes that the height does not change significantly between the application of the 8 gmf and the breaking point, one has a reasonable estimate of the actual wire geometry at the breaking pull strength. Careful specification of the loop geometry does not directly help to make better bonds, but it does help to minimize the uncertainties introduced by the pull test method of testing the bonds.

An initial try at bonding to 0.1 μm Al film was completely unsuccessful. No bonds could be made to stick. For the 1.6 μm film, and 25.4 μm wire, the bonding parameters were varied to determine a schedule which simultaneously yielded the maximum equal pull strength at both bonds with virtually all breaks on pull occurring at the bond heels. This condition is most easily reached by varying the schedule to minimize the bond squash factor while avoiding bond separation on pull. Using the optimum power settings, the differences between

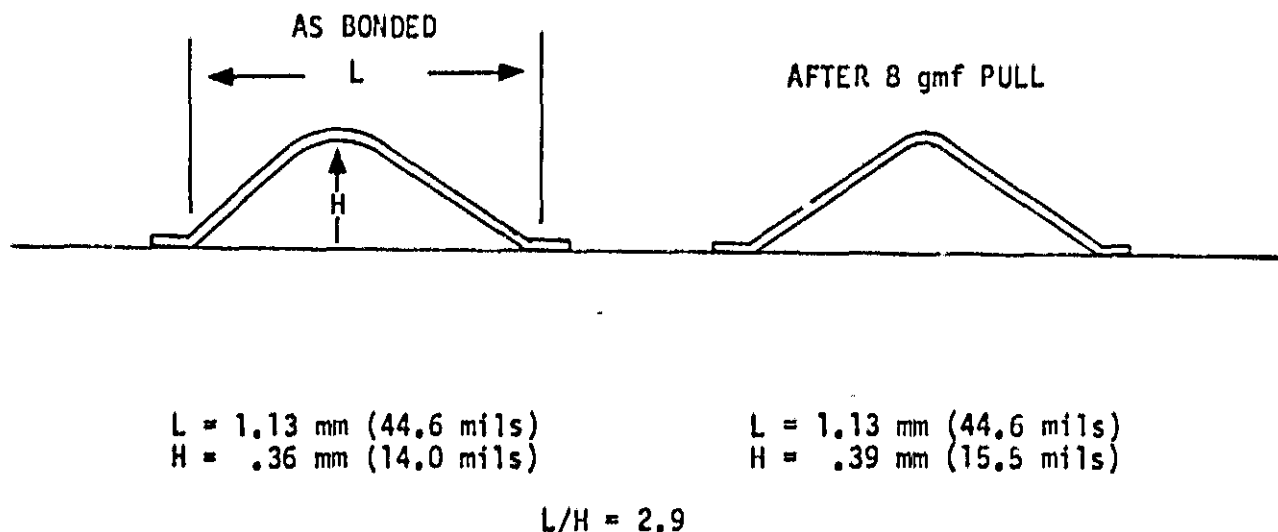


Figure 3-1. Wire Geometry

the 25, 27.5 and 30 gmf bond force settings were not very large. The 30 gmf force was selected based mostly on visual criteria. The squash factor with the optimum settings was quite high, approximately 2.5:1. This large factor is not generally regarded as desirable, but the data indicates no real disadvantage.

A similar attempt was made to develop an optimum schedule for bonding 38.1 μm wire to the aluminum film. The bonding forces investigated were 30, 35, and 40 gmf with bonding times of 30, 60, and 90 ms. Power was varied for each combination of force and time from a value low enough to produce poor adhesion to a value resulting in excessive squash factor. In all cases, the basic result was the same: no amount of variation of bonding parameters within the range indicated would produce optimum bonds. As the bonding motive (force, time, power) was increased, bond adhesion failures continued to occur until the bond foot was completely distorted.

The pull test data for the 25.4 μm Al wire on 1.6 μm Al film is shown in Table 3-9. The geometry results in a L/H ratio of 2.9, which means that from simple resolution of forces considerations, the actual tensile force in the wire at the breaking point is given by:

$$\text{Breaking Tensile Force} = 0.88 * \text{Pull Strength}$$

Heat soak produced a reduction in pull strength of about 22%, whereas 100 thermal cycles reduced it about 25% from the initial value.

3.6 BOND RESISTANCE

All of the samples that were investigated for electrical resistance had received heat soak and thermal cycling before the final resistance measurements were made, whether pull test data

was collected or not. Because the series paths shared the same bonding pads as the pull test jumpers, the first step in making the final resistance measurement was the breaking of all the jumpers that had not already been broken during pull testing. The location of the series paths placed many series bonds near the edge of the substrate, where they were very susceptible to handling damage. Therefore, damaged loops were removed and replaced. The samples on aluminum film were not subject to either problem.

The resistance data are shown in Table 3-10. The resistance change was quite small in all cases. This is not to say that all the series paths were continuous before the resistance measurements were made. The handling damage caused some opens which were repaired and could have masked others that might have occurred independently of the damage. In addition, a few opens were discovered during probing. These opens were not obvious under casual visual inspection, but were located by a combination of probing and the brush test.

The brush test is a simple technique for the non-destructive location of poor wire bonds. The technique was originated by our test technicians during troubleshooting of inoperative modules during pre-cap electrical test. The test consists of using a 00 artist's brush to brush the lower ends of the wire bonds. Wire movement is an indication of a bad bond. Measurement of the forces generated indicates that they are less than 2 gmf under the conditions of use.

Because of the difficulty in separating the different causes of opens, the data analysis was centered on the resistance of the mechanically continuous bonds.

**Table 3-1. Bond Strength Distribution, Thick Film Pattern,
25.4 μ m (1 mil) Wire**

	Initial	After 72 Hrs @ 150 °C	After Temperature Cycling -65 °C to +150 °C			
			10CS	20CS	60CS	100CS
Group A, 64 μm (2.5 mil) Bond Length						
Loops Pulled	370	370	370	185		
Mean (gmf)	8.2	4.0	3.96	4.4		
Std. Deviation (gmf)	2.15	1.46	1.05	1.22		
Maximum (gmf)	14	9	6	8		
Minimum (gmf)	2	2	2	2		
Coef. of Variation	26.2%	36.58%	26.25%	27.4%		
Group B, 76 μm (3 mil) Bond Length						
Loops Pulled	300	300				300
Mean (gmf)	11.5	5.6				4.7
Std. Deviation (gmf)	2.2	2.0				1.79
Maximum (gmf)	17	10				11
Minimum (gmf)	4	2				2
Coef. of Variation	19.1%	35.7%				38.1%
Group C, 76 μm (3 mil) Bond Length						
Loops Pulled	300	300	300		120	
Mean (gmf)	9.8	4.4	4.3		4.5	
Std. Deviation (gmf)	3.0	1.75	1.7		1.78	
Maximum (gmf)	16	8	9		9	
Minimum (gmf)	2	2	2		2	
Coef. of Variation	30.6%	39.8%	39.5%		39.5%	

**Table 3-2. Bond Strength Distribution, Thick Film Pattern,
38.1 μ m (1.5 mil) Wire**

	Initial	After 72 Hrs @ 150°C	After Temperature Cycling -65°C to +150°C			
			10CS	20CS	60CS	100CS
GROUP A						
Loops Pulled	370	370	370	185		
Mean (gmf)	14.4	8.4	9.0	7.7		
Std. Deviation (gmf)	2.94	3.0	3.0	3.28		
Maximum (gmf)	28	18	22	15		
Minimum (gmf)	2	2	2	3		
Coef. of Variation	20.4%	35.7%	33.3%	42.5%		
GROUP B						
Loops Pulled	300	300				300
Mean (gmf)	13.0	7.2				7.8
Std. Deviation (gmf)	2.75	2.9				2.94
Maximum (gmf)	20	15				17
Minimum (gmf)	4	2				3
Coef. of Variation	21.15%	40.3%				37.6%
GROUP C						
Loops Pulled	300	300	300		120	
Mean (gmf)	14.5	7.2	7.45		7.5	
Std. Deviation (gmf)	3.3	3.55	3.8		3.26	
Maximum (gmf)	22	17	18		17	
Minimum (gmf)	5	2	2		2	
Coef. of Variation	22.75%	49.3%	51.0%		43.5%	

**Table 3-3. Bond Strength Distribution, Thick Film Pattern,
50.8 μ m (2 mil) Wire**

	Initial	After 72 Hrs @ 150°C	After Temperature Cycling -65°C to +150°C			
			10CS	20CS	60CS	100CS
GROUP A						
Loops Pulled	370	370	370	185		
Mean (gmf)	30.85	17.6	18.4	15.6		
Std. Deviation (gmf)	8.04	6.04	5.9	5.6		
Maximum (gmf)	50	32	30	30		
Minimum (gmf)	5	4	5	6		
Coef. of Variation	26.05%	35.2%	32.1%	35.9%		
GROUP B						
Loops Pulled	300	300				300
Mean (gmf)	34.7	16.6				16.3
Std. Deviation (gmf)	7.35	6.5				5.71
Maximum (gmf)	50	32				32
Minimum (gmf)	10	5				4
Coef. of Variation	21.2%	39.1%				35.0%
GROUP C						
Loops Pulled	300	300	300		120	
Mean (gmf)	33.8	15.3	16.5		17.4	
Std. Deviation (gmf)	8.95	5.25	5.45		6.22	
Maximum (gmf)	59	29	29		29	
Minimum (gmf)	11	4	5		7	
Coef. of Variation	26.5%	34.3%	33.0%		35.7%	

Table 3-4. Bond Strength Distribution, Al Wire Bonded to Thick Film and Chips

	Initial	After 72 Hrs @ 150°C	After Temperature Cycling -65°C to +150°C 100CS
25.4 μ m (1 mil) Diameter Wire			
Loops Pulled	210	221	256
Mean (gmf)	9.9	5.5	5.1
Std. Deviation (gmf)	2.2	1.7	1.4
Maximum (gmf)	15	11	9
Minimum (gmf)	3	3	3
Failures (\leq 2 gmf)	1	4	4
Coef. of Variation	22.2%	31.1%	27.4%
38.1 μ m (1.5 mil) Diameter Wire			
Loops Pulled	222	219	135
Mean (gmf)	15.8	11.0	11.2
Std. Deviation (gmf)	2.2	2.2	2.6
Maximum (gmf)	24	17	16
Minimum (gmf)	10	5	5
Failures (\leq 4 gmf)	0	2	2
Coef. of Variation	14.0%	20.2%	23.3%

Table 3-5. Bond Strength Distribution, Thin Film Pattern,
25.4 μm (1 mil) Wire

	Initial	After 72 Hrs @ 150°C	After Temperature Cycling -65°C to +150°C			
			10CS	20CS	60CS	100CS
Group A1, 64 μm (2.5 mil) Bond Length						
Loops Pulled	70	70	60	60		
Mean (gmf)	7.5	5.1	5.2	4.4		
Std. Deviation (gmf)	2.2	1.2	0.88	1.0		
Maximum (gmf)	11	8	8	7		
Minimum (gmf)	2	2	3	2		
Coef. of Variation	29.3%	23.5%	16.9%	22.7%		
Group A2, 76 μm (3 mil) Bond Length						
Loops Pulled	270	270				
Mean (gmf)	11.5	7.7				
Std. Deviation (gmf)	2.75	1.90				
Maximum (gmf)	18	17				
Minimum (gmf)	3	3				
Coef. of Variation	23.9%	24.7%				
Group B, 76 μm (3 mil) Bond Length						
Loops Pulled	300	300				
Mean (gmf)	10.8	7.3				
Std. Deviation (gmf)	2.5	1.44				
Maximum (gmf)	16	11				
Minimum (gmf)	3	3				
Coef. of Variation	23.1%	19.7%				
Group C, 76 μm (3 mil) Bond Length						
Loops Pulled	300	300				300
Mean (gmf)	12.2	7.3				7.4
Std. Deviation (gmf)	1.75	1.23				1.91
Maximum (gmf)	16.0	10				18
Minimum (gmf)	6.0	4				3
Coef. of Variation	14.3%	16.8%				25.8%

**Table 3-6. Bond Strength Distribution, Thin Film Pattern,
38.1 μ m (1.5 mil) Wire**

	Initial	After 72 Hrs @ 150°C	After Temperature Cycling -65°C to +150°C			
			10CS	20CS	60CS	100CS
Group A						
Loops Pulled	310	340	60	60		
Mean (gmf)	13.8	15.6	11.6	12.1		
Std. Deviation (gmf)	4.05	2.98	3.86	4.72		
Maximum (gmf)	22	23	19	24		
Minimum (gmf)	4	5	4	5		
Coef. of Variation	29.3%	19.1%	33.4%	38.9%		
Group B						
Loops Pulled	300	300				
Mean (gmf)	13.5	12.7				
Std. Deviation (gmf)	4.4	5.18				
Maximum (gmf)	22	25				
Minimum (gmf)	4	4				
Coef. of Variation	32.6%	40.8%				
Group C						
Loops Pulled	300	300				300
Mean (gmf)	16.0	17.4				13.3
Std. Deviation (gmf)	4.07	3.18				4.63
Maximum (gmf)	23	25				25
Minimum (gmf)	5	8				4
Coef. of Variation	25.4%	18.2%				34.8%

**Table 3-7. Bond Strength Distribution, Thin Film Pattern,
50.8 μ m (2 mil) Wire**

	Initial	After 72 Hrs @ 150°C	After Temperature Cycling -65°C to +150°C			
			10CS	20CS	60CS	100CS
Group A						
Loops Pulled	340	340	60	60		
Mean (gmf)	44.2	31.5	30.6	25.2		
Std. Deviation (gmf)	6.5	7.91	8.5	6.3		
Maximum (gmf)	62	51	46	43		
Minimum (gmf)	18	15	14	8		
Coef. of Variation	14.7%	25.1%	27.8%	25.2%		
Group B						
Loops Pulled	300	300				
Mean (gmf)	45.6	28.9				
Std. Deviation (gmf)	9.3	6.17				
Maximum (gmf)	60	47				
Minimum (gmf)	20	14				
Coef. of Variation	20.4%	21.3%				
Group C						
Loops Pulled	300	300				300
Mean (gmf)	49.3	30.7				29.4
Std. Deviation (gmf)	6.7	6.74				7.6
Maximum (gmf)	64	50				47
Minimum (gmf)	18	16				8
Coef. of Variation	13.6%	22.0%				25.9%

**Table 3-8. Bond Strength Distribution, Al Wire Bonded
to Thin Film and Chips**

	Initial	After 72 Hrs @ 150 °C	After Temperature Cycling -65 °C to 150 °C 100CS	
			Undisturbed or Moderately Damaged	Heavily or Very Heavily Damaged
25.4 μm (1 mil) Diameter Wire				
Loops Pulled	248	276	79	89
Mean (gmf)	10.1	7.2	7.2	6.9
Std. Deviation (gmf)	2.0	1.1	1.3	1.3
Maximum (gmf)	14	11	10	11
Minimum (gmf)	3	3	5	4
Failures (≤ 2 gmf)	1	0	*	*
Coef. of Deviation	19.9%	19.8%	17.8%	18.2%
38.1 μm (1.5 mil) Diameter Wire				
Loops Pulled	248	246	250	
Mean (gmf)	15.7	13.3	13.4	
Std. Deviation (gmf)	2.5	2.2	2.1	
Maximum (gmf)	21	18	20	
Minimum (gmf)	6	5	5	
Failures (≤ 4 gmf)	1	0	1	
Coef. of Deviation	16.2%	16.7%	15.9%	

*Failures unrecorded.

**Table 3-9. Bond Strength Distribution, Al Wire Bonded
to 1.6 μ m Al Film**

	Initial	After 72 Hrs @ 150°C	After Temperature Cycling -65°C to +150°C 100 CS
Loops Pulled	250	250	250
Mean (gmf)	11.8	9.3	8.9
Std. Deviation (gmf)	.58	.61	.53
Maximum (gmf)	13	11	10.5
Minimum (gmf)	10	8	7
Failures (\leq 2 gmf)	0	0	0
Coef. of Deviation	4.9%	6.5%	6.0%

Table 3-10. Electrical Resistance Data

System	No. of Samples Measured	No. of Bonds Per Sample	Average Sample Resistance*		Change of Individual Samples
			After Bonding	After Thermal Soak & Thermal Cycle	
25.4 μ m Al Wire - Thick Film Au	13	198	14.26 \pm 1.09 Ω	14.34 \pm 1.04 Ω	Mixed + and -
38.1 μ m Al Wire - Thick Film Au	17	198	8.96 \pm 0.54 Ω	8.40 \pm 0.18 Ω	Predominantly -
50.8 μ m Al Wire - Thick Film Au	22	198	5.91 \pm 0.32 Ω	5.54 \pm 0.19 Ω	All -
25.4 μ m Al Wire - Thin Film Au	20	198	18.58 \pm 1.69 Ω	18.25 \pm 2.76 Ω	Mixed + and -
38.1 μ m Al Wire - Thin Film Au	19	198	9.84 \pm 0.45 Ω	11.06 \pm 0.57 Ω	All +
50.8 μ m Al Wire - Thin Film Au	19	198	7.99 \pm 0.69 Ω	9.59 \pm 1.01 Ω	All +
25.4 μ m Al Wire - 1.6 μ m Al Film	10	18	2.41 \pm 0.03 Ω	2.39 \pm 0.03 Ω	Mixed. The maximum individual change was 0.07 Ω

*In the form: Average \pm Std. Deviation

4. CONCLUSIONS

Several overall conclusions can be drawn from the data and observations made during the study.

- a. A reduction in pull strength of ultrasonically bonded aluminum wire after heat soak is normal, as a result of annealing of the wire itself. Even the Al wire bonded to Al film (where there is no possibility of alloy formation) showed a reduction of about 22% after heat soak and an additional 3% after thermal cycle.
- b. The 50.8 μm wire was relatively harder than either the 25.4 or the 38.1 μm wire. This conclusion is based on the observation of the relative squash factors of good bonds made with the three wire sizes, and the relative tensile strengths per unit cross section of the wire.
- c. The 38.1 μm wire was softer than optimum. This conclusion is based on the comparative tensile strengths per unit cross section, and also on the comparative bondability to the aluminum film. The relatively low initial strength, and the small overall reduction in strength due to thermal treatment when bonded to thin film gold, further substantiates this conclusion based on the idea that an initially softer wire will soften less relative to a hard one during thermal treatment.
- d. The pull strengths on 25.4 μm wire bonded to thin film gold were significantly higher when the tool with the longer foot length was used.
- e. In most cases, the thermal cycling had relatively little additional effect on the pull strengths beyond that already produced by the heat soak. It should be pointed out however that especially with the bonding to the thick- and thin-film gold, rather large loop heights ($0.75 < L/H < 2$) were used as is common in wire bonding to hybrids where adequate headroom is usually available. This minimizes the amount of flexing experienced by the bond heels during thermal cycle. Flexing is usually cited as the cause of bond failures due to thermal cycling.⁷
- f. Careful control of the measurement process as well as the materials, equipment, and bonding process must be maintained in order to achieve reliable results. The double-bond pull test has one element in its favor, namely it is simple to perform. However, uncertainties inherent to the test itself can introduce variations in the data in addition to the real variations in the bond strength. Even if the bond geometry is held constant, friction at the hook can still affect the results, especially in the bi-level system.
- g. The change in the resistance of mechanically stable bonds was small compared to the overall resistance due to the probe, the bonding pads, and the wire.

- h. The minimum bond strengths listed in Method 2011 of MIL-STD-883A for destructive bond pull test do not assure for ultrasonic bonding of small diameter aluminum wire that the bonding machine is properly adjusted and the bonding process is well controlled.
- i. Optimum schedule of bonding machine tool force and bonding time and power (bonding tool amplitude) must be uniquely determined for each machine setup.

4.1 THICK FILM GOLD

The thick film gold studied in this program would not be satisfactory for hybrids required to operate at elevated temperatures for extended periods of time. The bonding process itself was marginal for the $50.8\ \mu\text{m}$ film due to inadequate film adhesion, although the hard wire may have contributed to that problem. The major failing of the overall Al wire/thick-film gold system was that the adhesion of the wire to the film seriously degraded as a result of the heat treatment in all cases.

Figure 4-1A shows a SEM photo of a $25.4\ \mu\text{m}$ wire bonded to the thick film. On the basis of the appearance of the bond and the gold at the toe end, one might conclude that the interface between the gold and aluminum lies below the "surface" of the surrounding gold. But there is no evidence of the gold having been displaced laterally, which suggests that there are voids within the film as well as on the surface. Such voids could interfere with the proper coupling of power into the system. Another possibility might be that the presence of the glass frit in the gold interferes in some way detrimental to the bond strength, perhaps by providing some impurity that can segregate at the interface as a result of thermal treatment.

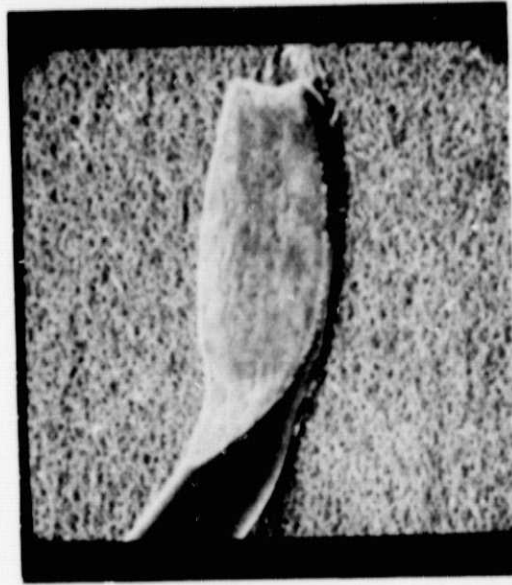
4.2 THIN FILM GOLD

The thin film gold did not exhibit the failure of adhesion characteristic of the thick film. However, if one uses the data from the thin film aluminum as a standard and assumes that the degradation there was all due to wire annealing, then the thin film gold suffered from 5 to 15% additional loss of strength for a total loss of from 30 to 40%. Observation of the failure mode indicates that the bonds themselves get stronger relative to the wire. This could be due to one of two mechanisms: Either the bonds actually got stronger by some heat related mechanism (perhaps by interdiffusion). This assumes that the temperature-time relationship was too low to cause Kirkendall voids. Or else the adhesive strength did not actually change, but degradation of the strength of the wire because of some heat related cause simply caused the heel to break before the adhesive limit of the bonds was reached. If the latter is true, then some other metallurgical change related to the specific combination of materials and certainly including the possible effects of impurities has to be involved in order to explain the greater strength loss compared to Al on Al.

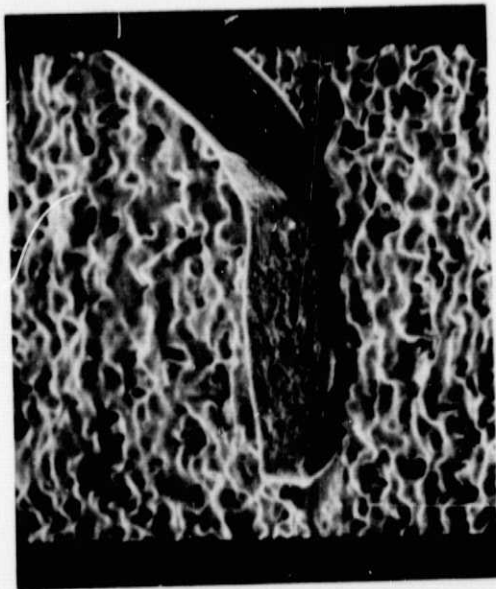
ORIGINAL PAGE IS
OF POOR QUALITY



B. THIN FILM GOLD, STANDARD SUBSTRATE



D. THIN FILM ALUMINUM, STANDARD SUBSTRATE



A. THICK FILM GOLD



C. THIN FILM GOLD, GLAZED SUBSTRATE

Figure 4-1. Wire Bonds (25.4 μm)

It has recently been pointed out by Joyce Gilliam that bonds to thin film gold on smoother substrates, namely $0.1\text{ }\mu\text{m}$ ($4\text{ }\mu\text{in.}$) alumina or glazed alumina ($0.025\text{ }\mu\text{m}$) ($1\text{ }\mu\text{in.}$) are generally easier to make and require lower squash factor than on the standard $0.25\text{ }\mu\text{m}$ substrates. The fact that the relatively thin aluminum ($1.6\text{ }\mu\text{m}$) on $0.25\text{ }\mu\text{m}$ substrates required the high squash factor and the thick film gold ($>11\text{ }\mu\text{m}$ thick on $0.63\text{ }\mu\text{m}$ substrate) required a squash factor roughly equal to the thin film gold ($2.5\text{ }\mu\text{m}$ thick on $0.25\text{ }\mu\text{m}$ substrate) indicates that the metal thickness as well as the wire hardness and substrate smoothness play important roles in optimizing the ultrasonic bond. Figures 4-1A thru 4-1D show $25.4\text{ }\mu\text{m}$ wires bonded to the thick film Au, thin film Au on as-fired and glazed alumina, and aluminum on as-fired alumina respectively.

4.3 CHIPS

The overall information on the bonding to chips is clouded by the limitations of the double-bond pull test. However, it is clear that at least in some cases, the bond to the chips separated from the metalization, which indicates that these chips at least were underbonded. No particular pattern of failure was observed. These chip pull-ups were almost universally on the low side of the mean and were frequently at or near the low edge of the distribution. In our production experience, the vast majority of bonding problems occur at the chip.

From the standpoint of materials and substrate smoothness, the chip should be the easiest point at which to make a bond. However, in the assembly of a hybrid, considerations of size of the chip bonding pad, provision for rework, precautions to prevent shorting to the silicon substrate, and variation in bondability from one chip to another actually makes it more difficult.

This emphasizes one of the problem areas for hybrid circuits. The ability to intermix in a single package many different kinds of components, frequently from different manufacturers or made by different processes, is one of the strengths of hybrids. But, at the same time, it is also a complicating factor because, for example, an optimum bonding schedule for one component may not be suitable for another. We have, on a few occasions, encountered chips from one manufacturer that were very difficult to bond. In such a case, the simplest solution is to use an electrically identical chip from another manufacturer. In another case however, we became a second source for certain hybrid (and ultimately the prime source) because another hybrid manufacturer was not able to bond to a certain high-performance single-source family of IC chips. In this case, we were able to bond to these chips, but not without difficulty.

The manufacturers of chips develop processes which meet their quality requirements for packaged devices, which are their major source of income. They can even adjust the bonding process to compensate for differences in the characteristics of different families. However, to our knowledge, little comparative information is available to guide hybrid manufacturers in this area.

4.4 THIN FILM ALUMINUM

The results of bonding to thin film aluminum were excellent. By carefully controlling the geometry and the bonding schedule, very tight distributions were obtained. In addition, the degradation of the bond pull strength with thermal treatment was less than with either the thick or thin film gold. The lowest pull strength measured, even after heat soak and thermal cycling, was 7 gmf.

The theoretical reliability advantages of a monometallic hybrid conductor system are obvious. Certain areas would require further investigation before such a system could be put into use. The compatibility of the aluminum as a termination for Ni/Cr on a relatively rough substrate would have to be determined, as well as a selective etching method for the aluminum that would be compatible with the Ni/Cr resistors.

5. RECOMMENDATIONS

Recommendations, based on the work performed, are as follows:

1. Timing on K&S 484 bonders should be checked to ensure that the generator does not fire before the bonding force has stabilized.
2. Implement the complete NBS calibration procedure for wire bonding machines. This includes the use of tool amplitude calibration on at least a daily basis, and after any disturbance of the bonding tool.
3. In addition to the regular Q.C. checking of bond strength for machine and operator, the operator should make and pull bonds daily to provide direct feedback of the result of work performed. The standard deviation should not exceed 15% in a group of bonds, with a minimum allowable value of 5 gmf for 25.4 μ m wire.
4. For test bonding, establish bond geometry control compatible with the purpose for which the test is being run (i.e., rather simple controls for daily tests, but carefully designed layouts for schedule establishment and materials and process evaluations to minimize the sensitivity of the data to the geometry).
5. All evaluations should include pull tests both before and after heat soak. On the other hand, thermal cycling would not be necessary in all cases, but only as a final check on the best materials and process combinations.
6. The foot length on bonding tools should be as long as practical within the limitations of the size of the bonding pad available.
7. All incoming bonding tools should be given visual inspection before use.
8. Evaluation of metallization bondability should ideally include effects of wire hardness, substrate smoothness, and metal thickness and impurities.
9. Fritless gold thick film materials should be evaluated.
10. A large scale, systematic study of bondability of semiconductor chips (hopefully with the cooperation with the chip manufacturers) should be run to provide guidelines for reliable bonding to these widely variable components.
11. A development program for a Ni/Cr - aluminum hybrid process should be implemented.

6. REFERENCES

1. Harman, G.G., and Leedy, K.O., "An Experimental Model of the Microelectronic Ultrasonic Wire Bonding Mechanism", Proceedings of the 1972 IEEE Reliability Physics Symposium, Las Vegas, 1972, pp 49-56.
2. National Bureau of Standards, NBS Special Publication 400-2, Microelectronic Ultrasonic Bonding, G.G. Harman, ed, January 1974, p 29.
3. Unger, R.F., Aluminum Ribbon and Round Wire Bonding: Comparative Analysis, NELC Technical Report 1946, March 1975, p 5.
4. Reference 3, p 11.
5. Reference 2, p 49.
6. Reference 2, p 20.
7. Ravi, K.V., and Philofsky, E.M., "Reliability Improvement of Wire Bonds Subjected to Fatigue Stress", Proceedings of the 1972 IEEE Reliability Physics Symposium, Las Vegas, 1972, p 143.